

A Full DAG Score-Based Algorithm for Learning Causal Bayesian Networks with Latent Confounders

Christophe Gonzales and Amir-Hosein Valizadeh

Aix Marseille Univ, CNRS, LIS, Marseille, France
christophe.gonzales@lis-lab.fr, amir.valizadeh@lis-lab.fr

Abstract. Causal Bayesian networks (CBN) are popular graphical probabilistic models that encode causal relations among variables. Learning their graphical structure from observational data has received a lot of attention in the literature. When there exists no latent (unobserved) confounder, i.e., no unobserved direct common cause of some observed variables, learning algorithms can be divided essentially into two classes: constraint-based and score-based approaches. The latter are often thought to be more robust than the former and to produce better results. However, to the best of our knowledge, when variables are discrete, no score-based algorithm is capable of dealing with latent confounders. This paper introduces the first fully score-based structure learning algorithm searching the space of DAGs (directed acyclic graphs) that is capable of identifying the presence of some latent confounders. It is justified mathematically and experiments highlight its effectiveness.

1 Introduction

Causal networks, a.k.a. causal Bayesian networks (CBN) [15], are graphical probabilistic models that encode cause-and-effect relationships. Like Bayesian networks (BN), they are constituted by i) a directed acyclic graph (DAG) whose nodes represent random variables and whose edges encode their relationships; and ii) a set of conditional probability distributions of the nodes/random variables given their parents in the graph. However, unlike BNs, the semantics of the edges is not merely correlation but rather a causal relationship, that is, an arc from A to B states that A is a direct cause of B . CBNs are important for Artificial Intelligence because they enable to perform the same kind of reasoning as humans do, in particular counterfactual reasoning (if I had done this, what would have happened?).

Although it is well-known that learning the structure of CBNs from only (observational) data is theoretically not always possible [15], many algorithms have been proposed in the literature for this purpose. When there exists no unmeasured *confounder*, i.e., no unobserved direct common cause of some measured variables, they can be essentially divided into two classes: constraint-based and score-based approaches. The former [20, 16, 4, 30] rely on statistical conditional independence tests to uncover the independence properties underlying the probability distribution that generated the data, thereby learning the graphical structure of the causal model. These methods are often not able to uncover the whole DAG of the CBN, so they provide weaker information in the form of a Completed Partially Directed Acyclic Graph (CPDAG). In such a graph, only the directed edges represent “true” causal relations, the undirected ones representing correlations, their causal direction remaining unknown. On

the other hand, score-based approaches [3, 6, 26] identify the DAG of the CBN as the one maximizing some fitness criterion on the data. They rely on either approximate or exact optimization techniques to uncover the searched DAG. However the orientations of its arcs may not always have a causal meaning. So this DAG is mapped into the CPDAG of its Markov equivalence class, which is the best that can be extracted in terms of causality from the data. Score-based approaches are usually considered more robust than constraint-based approaches, notably because, in the latter, errors in statistical tests can chain and decrease significantly the quality of the resulting CPDAGs.

However, in most practical situations, some variables play an important role in the causal mechanism and, yet, for different reasons, they are not or cannot be observed in the data. For instance, their measuring may be too expensive or it would require unethical processes. Constraint-based methods have been successfully extended to cope with such latent (unobserved) variables [5, 21, 31]. For score-based algorithms, it is somewhat different: it is commonly admitted that they are unable to cope with latent variables because they rely on searching for DAGs and DAGs are inadequate in the presence of latent variables. An extension of DAGs called Maximal Ancestral Graphs (MAG) [18] has been introduced precisely to fix this issue and score-based approaches have been adapted to learn MAGs [17, 13, 23]. Unfortunately, currently, they can only cope with scoring MAGs over continuous variables. Yet, this is restrictive because there exist situations in which variables are discrete by nature and cannot be meaningfully extended as continuous ones, e.g., non-ordinal variables such as colors, locations, types of devices, *etc.*

In this paper, we address problems in which all the random variables are discrete. In [22], it was shown that causal models with arbitrary latent variables can always be converted into semi-Markovian causal models (SMCM), i.e., models in which latent variables have no parent and only two children, while preserving the same independence relations between the observed variables. So, to deal with latent confounders, we focus on learning SMCMs. More precisely, we show that, without any prior knowledge about the latent confounders or their number, DAGs learnt from observational data by latent confounders-unaware score-based approaches encode sufficient information to recover many latent confounders and their locations. Exploiting this property, we provide and justify a structure learning algorithm that i) only relies on scores; ii) uses only DAGs; and iii) is capable of identifying some latent confounders and their locations.

The rest of the paper is organized as follows. Section 2 presents formally causal models and some algorithms for learning BN and/or CBN structures from observational data that can cope with latent

confounders. Then, in Section 3, we introduce our new algorithm and justify why it is capable of identifying latent confounders. Its effectiveness is highlighted through experiments in Section 4. Finally a conclusion and some future works are provided in Section 5.

2 Causal Models and Structure Learning

In the paper, bold letters represent sets. \mathbf{X} denotes a set *discrete* random variables. For a directed graph \mathcal{G} , $\mathbf{Ch}_{\mathcal{G}}(X)$ and $\mathbf{Pa}_{\mathcal{G}}(X)$ denote the set of children and parents of node X respectively, i.e., the set of nodes Y such that there exists an arc from X to Y and from Y to X respectively. A causal model over \mathbf{X} is defined as follows [15]:

Definition 1. A causal model is a pair (G, Θ) where $G = (\mathbf{X}, \mathcal{E})$ is a DAG¹ and \mathcal{E} is a set of arcs. To each $X_i \in \mathbf{X}$ is assigned a random disturbance ξ_i . $\Theta = \{f_i(\mathbf{Pa}_{\mathcal{G}}(X_i), \xi_i)\}_{X_i \in \mathbf{X}} \cup \{P(\xi_i)\}_{X_i \in \mathbf{X}}$, where f_i 's are functions assigned to X_i 's and P are probability distributions over disturbances ξ_i .

It is easy to see² that a causal model can be represented equivalently by a Bayesian network – BN [14]:

Definition 2. A BN is a pair (G, Θ) where $G = (\mathbf{X}, \mathcal{E})$ is a directed acyclic graph (DAG), \mathbf{X} represents a set of random variables, \mathcal{E} is a set of arcs, and $\Theta = \{P(X|\mathbf{Pa}_{\mathcal{G}}(X))\}_{X \in \mathbf{X}}$ is the set of the conditional probability distributions (CPD) of the nodes / random variables X in \mathcal{G} given their parents $\mathbf{Pa}_{\mathcal{G}}(X)$ in \mathcal{G} . The BN encodes the joint probability over \mathbf{X} as $P(\mathbf{X}) = \prod_{X \in \mathbf{X}} P(X|\mathbf{Pa}_{\mathcal{G}}(X))$.

Causal models impose that the arcs are oriented in the direction of causality, that is, an arc $X \rightarrow Y$ means that X is a direct cause of Y . In this case, the BN is called a CBN. In general, BNs do not impose this restriction since they only model probabilistic dependences. Hence a BN containing only Arc $X \rightarrow Y$ is equivalent to one containing Arc $Y \rightarrow X$. More precisely, the independence model of a BN is specified by the d -separation criterion [14]:

Definition 3 (Trails and d -separation). Let \mathcal{G} be a DAG. A trail C between nodes X and Y is a sequence of nodes $\langle X_1 = X, \dots, X_k = Y \rangle$ such that, for every $i \in \{1, \dots, k-1\}$, \mathcal{G} contains either Arc $X_i \rightarrow X_{i+1}$ or Arc $X_i \leftarrow X_{i+1}$.

Let \mathbf{Z} be a set of nodes disjoint from $\{X, Y\}$. X and Y are said to be d -separated by \mathbf{Z} , which is denoted by $\langle X \perp_{\mathcal{G}} Y | \mathbf{Z} \rangle$, if, for every trail C between X and Y , there exists a node $X_i \in C$, $i \notin \{1, k\}$, such that one of the following two conditions holds:

1. $\langle X_{i-1}, X_i, X_{i+1} \rangle$ is a collider, i.e., \mathcal{G} contains Arcs $X_{i-1} \rightarrow X_i$ and $X_i \leftarrow X_{i+1}$. In addition, neither X_i nor its descendants in \mathcal{G} belong to \mathbf{Z} . The descendants of a node are defined recursively as the union of its children and the descendants of these children.
2. $\langle X_{i-1}, X_i, X_{i+1} \rangle$ is not a collider and X_i belongs to \mathbf{Z} .

Such trails are called blocked, else they are active. Let $\mathbf{U}, \mathbf{V}, \mathbf{Z}$ be disjoint sets of nodes. Then \mathbf{U} and \mathbf{V} are d -separated by \mathbf{Z} if and only if X and Y are d -separated by \mathbf{Z} for all $X \in \mathbf{U}$ and all $Y \in \mathbf{V}$.

Let $\mathbf{U}, \mathbf{V}, \mathbf{Z} \subseteq \mathbf{X}$ be disjoint sets and let P be a probability distribution over \mathbf{X} . We denote by $\mathbf{U} \perp_{\mathcal{P}} \mathbf{V} | \mathbf{Z}$ the probabilistic conditional independence of \mathbf{U} and \mathbf{V} given \mathbf{Z} . The independence model of BNs is the following:

$$\langle \mathbf{U} \perp_{\mathcal{G}} \mathbf{V} | \mathbf{Z} \rangle \implies \mathbf{U} \perp_{\mathcal{P}} \mathbf{V} | \mathbf{Z}. \quad (1)$$

¹ By abuse of notation, we use interchangeably $X \in \mathbf{X}$ to denote a node in the model and its corresponding random variable.

² See the supplementary material, Appendix C, at the end of the paper.

Two BNs with the same set of d -separation properties therefore represent the same independence model. Any graphical model satisfying Eq. (1) is called an I-map (*independence map*). The d -separation criterion implies that two BNs represent the same independence model if and only if they have the same *skeleton* and the same set of *v-structures* [29]: the skeleton of a directed graph \mathcal{G} is the undirected graph obtained by removing all the orientations from the arcs of \mathcal{G} ; *v-structures* are colliders $\langle X_{i-1}, X_i, X_{i+1} \rangle$ such that \mathcal{G} does not contain any arc between X_{i-1} and X_{i+1} . The directions of the arcs in *v-structures* are therefore identical for all BNs that represent the same sets of independences. When Eq. (1) is substituted by:

$$\langle \mathbf{U} \perp_{\mathcal{G}} \mathbf{V} | \mathbf{Z} \rangle \iff \mathbf{U} \perp_{\mathcal{P}} \mathbf{V} | \mathbf{Z}, \quad (2)$$

then the graphical model is called a P-map (*perfect map*).

To learn the structure of a BN from observational data, it is usually assumed that the distribution P that generated the data has a P-map (although there exist some papers that relax this assumption [16, 10, 11]). Then, it is sufficient to learn the independence model of the data (the set of conditional independences): each independence $X \perp_{\mathcal{P}} Y | \mathbf{Z}$ necessarily implies the lack of an arc between X and Y in the BN. The (undirected) edges of the skeleton therefore correspond to all the pairs of nodes (X, Y) for which no conditional independence was found. The set of *v-structures* $\langle X, Z, Y \rangle$ is the set of triples (X, Z, Y) such that i) edges $X - Z$ and $Z - Y$ belong to the skeleton and ii) there exist sets $\mathbf{Z} \not\supseteq \{Z\}$ such that $X \perp_{\mathcal{P}} Y | \mathbf{Z}$. The edges of the skeleton corresponding to *v-structures* can be oriented accordingly. Now, to avoid creating additional spurious *v-structures* or directed cycles (which are forbidden in DAGs), some edges need necessarily be oriented in a given direction. These are identified using Meek's rules [12] and can be computed in polynomial time [2]. The graph resulting from all these orientations is called a CPDAG (*Completed Partially Directed Acyclic Graph*). To complete the learning of the BN's structure, there just remains to orient the remaining undirected edges. To do so, it is sufficient to sequentially apply the following two operations until there remains no undirected edge: i) orient in any direction one (arbitrary) edge; and ii) apply Meek's rules. This is precisely what *constraint-based* algorithms like PC [20], PC-stable [4], CPC [16], IC [29] or FCI [21] do, relying on statistical independence tests. MIIC [30] essentially performs the same operations but exploiting multivariate information instead.

There exist many other algorithms, based notably on learning Markov blankets [25] or on scoring DAGs [6, 8, 3, 26]. The key idea of score-based approaches is to assign to each DAG a score representing its fitness on the data. Under some assumptions, the one maximizing this criterion is the one that generated the data. In the rest of the paper, we exploit the BIC score [19]:

$$S(X|\mathbf{Z}) = \sum_{x \in \Omega_X} \sum_{\mathbf{z} \in \Omega_{\mathbf{Z}}} N_{x\mathbf{z}} \log \left(\frac{N_{x\mathbf{z}}}{N_{\mathbf{z}}} \right) - \frac{1}{2} \log(|\mathcal{D}|) \dim(X|\mathbf{Z}),$$

where $S(X|\mathbf{Z})$ denotes the score of node X given parent set \mathbf{Z} ; Ω_X and $\Omega_{\mathbf{Z}}$ represent the domains of X and \mathbf{Z} respectively; $N_{x\mathbf{z}}$ is the number of records in Database \mathcal{D} such that $X = x$ and $\mathbf{Z} = \mathbf{z}$; $N_{\mathbf{z}} = \sum_{x \in \Omega_X} N_{x\mathbf{z}}$; and, finally, $\dim(X|\mathbf{Z})$ is the number of free parameters in the conditional probability distribution $P(X|\mathbf{Z})$, i.e., $\dim(X|\mathbf{Z}) = (|\Omega_X| - 1) \times |\Omega_{\mathbf{Z}}|$. The term $\frac{1}{2} \log(|\mathcal{D}|) \dim(X|\mathbf{Z})$ is called the *penalty* of the score.

In the literature, *v-structures* are considered to represent causal relations, that is, the directions of their arcs have a causal meaning. This implies that, when there exist no latent confounder, CPDAGs are precisely the best that can be extracted in terms of causality from the

data. So, all the aforementioned algorithms do actually learn CBNs when they return CPDAGs instead of full BNs.

In practice, for different reasons (ethics, price, immeasurability, etc.), it is often the case that some confounders cannot be observed. Constraint-based approaches, notably FCI, have been extended to deal with such situations. Instead of returning a CPDAG, they provide more informative graphs like Partial Ancestral Graphs (PAG) [17, 21]. PAGs are constituted by usual arcs (\rightarrow) but also labeled edges ($\circ-\circ$, $\circ\rightarrow$) and bidirected arcs (\leftrightarrow). The latter indicate the presence of a confounder, that is, $A \leftrightarrow B$ in a PAG means that there exists $A \leftarrow L \rightarrow B$ in the generating DAG, with L the confounder. The \circ labels indicate that the learning algorithm is uncertain whether there should be an arrow head or not, i.e., $\circ-$ is equivalent to either \leftarrow or $-$. For continuous random variables, score-based approaches have been extended to cope with latent confounders [17]. But, to our knowledge, when variables are discrete, there exists no score-based approach capable of dealing with latent confounders. One reason is that it is believed that detecting confounders is impossible when searching with scores the space of DAGs. We show in the next section that it is not the case.

3 A New Full Score-based Causal Learning Algorithm

In the rest of the paper, \mathbf{X} is divided into \mathbf{X}_O and \mathbf{X}_H , which represent sets of observed and hidden (latent) variables respectively. We assume that there exists an underlying probability distribution P^* over $\mathbf{X} = \mathbf{X}_O \cup \mathbf{X}_H$ that generated a dataset \mathcal{D}^* . But, as the variables in \mathbf{X}_H are unobserved (they are the latent confounders), only the projection \mathcal{D} of \mathcal{D}^* over \mathbf{X}_O , i.e., the dataset resulting from the removal from \mathcal{D}^* of all the values of the variables of \mathbf{X}_H , is available for learning. In addition, we assume that P^* is decomposable according to some DAG \mathcal{G}^* . The goal is to recover \mathcal{G}^* .

The key idea of our algorithm is summarized on Figure 1: the left side displays part of Graph \mathcal{G}^* , which contains a latent confounder $L \in \mathbf{X}_H$ and represents the structure of the causal network that generated the data; Graph \mathcal{G} on the right should be the one learnt by a score-based algorithm. Indeed, in \mathcal{G}^* , there exists no set $\mathbf{Z} \subseteq \mathbf{X}_O$ that d -separates A and B (because Trail $\langle A, L, B \rangle$ is active). Hence, provided \mathcal{G}^* is a P-map, A and B should be dependent and a structure with an arc between A and B should have a higher score than one without. Assume that this arc is $A \rightarrow B$. For the same reason, a structure with an arc between A and C (resp. B and D) should have a higher score than one without. Now, given any $\mathbf{Z} \supseteq \{A\}$, node B is not d -separated from C in \mathcal{G}^* because Trail $\langle C, A, L, B \rangle$ is active. But it would be on Fig. 1.b if there were no arc between B and C . This is the reason why score-based algorithms tend to produce structures with such an arc and analyzing such triangles (A, B, C) in the learnt graph should provide some insight on the location of the latent confounders. This intuition is confirmed by the next proposition.

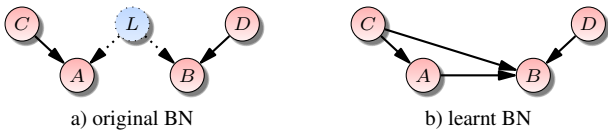


Figure 1: Triangles induced by latent confounders.

Proposition 1. Assume that there exists a perfect map $\mathcal{G}^* = (\mathbf{X}, \mathcal{E})$ for Distribution P^* and that \mathbf{X}_H is the set of latent confounders, i.e., all the nodes of \mathbf{X}_H have no parent and exactly two children in \mathcal{G}^* , which both belong to \mathbf{X}_O .

Let $L \in \mathbf{X}_H$ be any variable such that both of its children A, B in \mathcal{G}^* have at least one parent in \mathbf{X}_O . Then, if \mathcal{G} is a DAG maximizing the BIC score over \mathcal{D} , as $|\mathcal{D}| \rightarrow \infty$, \mathcal{G} contains an arc between A and B . Without loss of generality, assume this is Arc $A \rightarrow B$. Then, for every $C \in \text{Pa}_{\mathcal{G}^*}(A) \cap \mathbf{X}_O$, (A, B, C) is a clique in \mathcal{G} .

Proof: All the proofs are provided in the supplementary material, Appendix A, at the end of the paper. ■

Note that, in Proposition 1, both A and B have other parents than L . This is important because, as shown in Proposition 2 below, whenever node L is the only parent of A (resp. B), no learning algorithm can distinguish between a graph \mathcal{G}^* with a latent confounder L whose children are A and B (Fig. 2.a & 2.b), and a graph \mathcal{G}^* without latent confounder L but with an arc $A \rightarrow B$ (resp. $B \rightarrow A$) (Fig. 2.c). Similarly, as shown in Proposition 3, it is impossible to distinguish between a graph \mathcal{G}^* containing both latent confounder L and Arc $A \rightarrow B$ (Fig. 2.d), and a graph \mathcal{G}^* without latent confounder L but with both arcs $A \rightarrow B$ and $C \rightarrow B$ (Fig. 2.e).

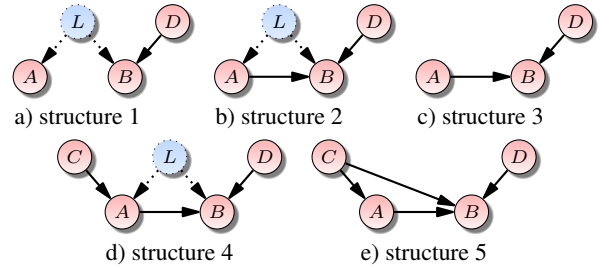


Figure 2: Some indistinguishable structures.

Proposition 2. Let $\mathcal{B}^* = (\mathcal{G}^*, \Theta)$ be a Bayesian network, with $\mathcal{G}^* = (\mathbf{X}, \mathcal{E})$. Let $L \in \mathbf{X}_H$ be such that $\text{Ch}_{\mathcal{G}^*}(L) = \{A, B\} \subseteq \mathbf{X}_O$ and $\text{Pa}_{\mathcal{G}^*}(L) = \emptyset$. In addition, assume that $\text{Pa}_{\mathcal{G}^*}(A) = \{L\}$. Finally, let \mathcal{G} be the graph resulting from the removal of L (and its outgoing arcs) from \mathcal{G}^* and the addition of arc $A \rightarrow B$ (if \mathcal{G}^* does not already contain it). Then, for any triple of disjoint subsets of variables $\mathbf{U}, \mathbf{V}, \mathbf{W}$ of \mathbf{X}_O , we have that:

$$\langle \mathbf{U} \perp_{\mathcal{G}} \mathbf{V} | \mathbf{W} \rangle \iff \langle \mathbf{U} \perp_{\mathcal{G}^*} \mathbf{V} | \mathbf{W} \rangle. \quad (3)$$

Proposition 3. Let $\mathcal{B}^* = (\mathcal{G}^*, \Theta)$ be a Bayesian network such that $\mathcal{G}^* = (\mathbf{X}, \mathcal{E})$ and Arc $A \rightarrow B$ belongs to \mathcal{E} . Let $L \in \mathbf{X}_H$ be such that $\text{Ch}_{\mathcal{G}^*}(L) = \{A, B\} \subseteq \mathbf{X}_O$. Finally, let \mathcal{G} be the graph resulting from the removal of L (and its outgoing arcs) from \mathcal{G}^* and the addition the set of arcs $\{X \rightarrow B : X \in \text{Pa}_{\mathcal{G}^*}(A) \setminus \{L\}\}$ (if \mathcal{G}^* does not already contain them). Then, for any triple of disjoint subsets of variables $\mathbf{U}, \mathbf{V}, \mathbf{W}$ of \mathbf{X}_O , we have that:

$$\langle \mathbf{U} \perp_{\mathcal{G}} \mathbf{V} | \mathbf{W} \rangle \iff \langle \mathbf{U} \perp_{\mathcal{G}^*} \mathbf{V} | \mathbf{W} \rangle. \quad (4)$$

In the two situations mentioned above, algorithms like FCI deal with indistinguishability by not choosing a single structure to return but rather by labelling arcs with \circ to highlight the uncertainty about the locations of the arrow heads and by asking the user to personally select which structure seems the most appropriate. In a sense, this corresponds to completing the structure learning with some user's expert knowledge. Other algorithms like MIIC or our algorithm prefer to choose which structure seems the best, hence relieving the user of such a burden. The rule followed by our algorithm is to discard latent variables when they are not absolutely necessary (i.e., in Fig. 2, it selects only Graphs 2.c & 2.e). This criterion can be viewed as a

simple Occam razor. So, without loss of generality, in the rest of the paper, we assume that i) there exists no arc between A and B in \mathcal{G}^* ; and ii) both A and B have other parents than L in \mathcal{G}^* .

The rationale of our algorithm relies on first learning a structure using any score-based algorithm and, second, examining the triangles to discover the latent confounders. The learnt DAG is then updated to take into account these confounders, mapping Fig. 1.b into Fig. 1.a. Unfortunately, the original network \mathcal{G}^* may itself contain some triangles, which we will call *genuine* triangles. So, we need to discriminate them from the ones induced by the latent confounders, which we call *latent* triangles. For this purpose, remark that, for every pair (X, Y) of variables of the genuine triangles, there exists no set $\mathbf{Z} \subseteq \mathbf{X}_O \setminus \{X, Y\}$ such that $\langle X \perp_{\mathcal{G}^*} Y | \mathbf{Z} \rangle$ because, \mathcal{G}^* containing an arc between X and Y , Trail $\langle X, Y \rangle$ is active. So, if \mathcal{G}^* is a perfect map and Dataset \mathcal{D} is sufficiently large, we should not find any $\mathbf{Z} \subseteq \mathbf{X}_O \setminus \{X, Y\}$ such that $X \perp_{P^*} Y | \mathbf{Z}$. Here, note that Dataset \mathcal{D} being the projection of \mathcal{D}^* on \mathbf{X}_O , it is generated by a distribution P over \mathbf{X}_O defined as the marginal of P^* over \mathbf{X}_O , i.e., $P = \sum_{\mathbf{X}_H} P^*$. But since \mathbf{X}_O contains $\{X\}$, $\{Y\}$ and \mathbf{Z} , joint probability $P(X, Y, \mathbf{Z}) = P^*(X, Y, \mathbf{Z})$, so that $X \perp_{P^*} Y | \mathbf{Z}$ is equivalent to $X \perp_P Y | \mathbf{Z}$. Overall, in Dataset \mathcal{D} , for genuine triangles, it should not be possible to find any pair of variables (X, Y) in the triangle such that there exists a set $\mathbf{Z} \subseteq \mathbf{X}_O \setminus \{X, Y\}$ such that $X \perp_P Y | \mathbf{Z}$.

In latent triangles, for the same reason, this property holds for pair (A, C) . For Pair (A, B) , it also holds because Trail $\langle A, L, B \rangle$ is active for all $\mathbf{Z} \subseteq \mathbf{X}_O \setminus \{A, B\}$ (see Fig. 1.a). On the contrary, for pair (B, C) of Fig. 1.b, there exist d -separating sets $\mathbf{Z} \subseteq \mathbf{X}_O \setminus \{B, C\}$ in \mathcal{G}^* because \mathcal{G}^* does not contain any arc between B and C . Note that $A \notin \mathbf{Z}$ otherwise Trail $\langle B, L, A, C \rangle$ of Fig. 1.a would be active and, so, $\langle B \not\perp_{\mathcal{G}^*} C | \mathbf{Z} \rangle$. So, in terms of independences observable in Dataset \mathcal{D} , there exist $\mathbf{Z} \subseteq \mathbf{X}_O \setminus \{A, B, C\}$ such $B \perp_P C | \mathbf{Z}$ and, moreover, $B \not\perp_P C | \mathbf{Z} \cup \{A\}$. This suggests the following property to discriminate between latent and genuine triangles:

Rule 1. *Only latent triangles contain exactly one pair of nodes that are independent given some set $\mathbf{Z} \subseteq \mathbf{X}_O$ but are dependent given \mathbf{Z} union the third node of the triangle.*

For the case of Fig. 1.a, any of the latent triangles of Fig. 3 can be learnt by score-based approaches because they encode exactly the same d -separation properties. In Fig. 3, the independent pair of nodes mentioned in Rule 1 is (B, C) for the three types. Triangles of types 2 and 3 share the fact that \mathcal{G}^* 's arc $A \rightarrow C$ has been reversed. If C had parents in \mathcal{G}^* , then these have become its children in \mathcal{G} to avoid creating new v -structures. So, when triangles of types 2 or 3 are learnt, C should not have many parents other than A , which may not be the case for B . So, to minimize the BIC score's penalty induced by the arc between B and C , the latter will most probably be oriented as $B \rightarrow C$. This intuition was confirmed in experiments we conducted: Type 2 triangles only allowed us to determine less than 0.5% of the latent confounders³. So, to speed-up our algorithm without decreasing significantly its effectiveness, we chose to exploit only Types 1 and 3 latent triangles. Note that this makes our algorithm only approximate but, as shown in the experiments, it still remains very effective. Rule 2 summarizes the features of the above triangles:

³ Note that, from an observational point of view, it is possible to discriminate between Type 2 and Type 3 triangles: in the former, C is a parent of B (as in the original graph \mathcal{G}^*). So, for parents D of B in \mathcal{G}^* , $\langle C, B, D \rangle$ is a v -structure in \mathcal{G} , which fits the independences observable in the dataset. On the contrary, in Type 3 triangles, the connection $\langle C, B, D \rangle$ is not a v -structure, which contradicts the observable independences. So, as shown in Figure 4, the learning algorithm should add an arc between D and C .

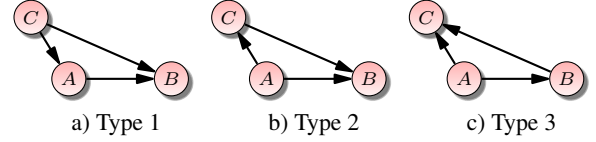


Figure 3: Possibly learnt latent triangles. For the three types, the independent pair of nodes mentioned in Rule 1 is (B, C) .

Rule 2. *Triangles of Type 1 and Type 3 are such that $C \rightarrow A \rightarrow B$ and $A \rightarrow B \rightarrow C$ respectively.*

For both types, there exists some set $\mathbf{Z} \subseteq \mathbf{X}_O \setminus \{A, B, C\}$ such that $B \perp_P C | \mathbf{Z}$ and $B \not\perp_P C | \mathbf{Z} \cup \{A\}$; and there exists no $\mathbf{Z} \subseteq \mathbf{X}_O \setminus \{A, B, C\}$ such that $A \perp_P B | \mathbf{Z}$ or $A \perp_P C | \mathbf{Z}$.

If score-based algorithms never made any mistake in their learning, we could simply use Rule 1 to identify latent triangles and the location of the latent confounders. However, in practice, similarly to constraint-based methods, they do make mistakes, which may induce our algorithm to incorrectly identify spurious latent triangles. Fortunately, it is possible to increase the robustness of the latent triangles identification by not only considering the dependences between nodes A , B and C but also by taking into account those involving node D , the parent of B in \mathcal{G}^* (See Fig. 1.a).

The dotted arcs in Fig. 4 are those involving D and nodes A , B , C that should be learnt by the score-based algorithm. In Type 1 triangles, there should therefore exist an arc $D \rightarrow B$, which can be translated as “node B must have at least 3 parents in \mathcal{G} ”. Triangles of Type 1 are therefore considered as latent only if they satisfy both this property and Rule 2. For Type 3 triangles, the situation is more complex because, in addition to Arc $D \rightarrow B$, there should also exist an arc between D and C to account for $\langle D \not\perp_{\mathcal{G}^*} C | \{A, B\} \rangle$. Note that Triangle (D, B, C) cannot be misinterpreted as latent because both pairs (B, C) and (C, D) can be made independent given some $\mathbf{Z} \subseteq \mathbf{X}_O$, hence ruling out Rule 1. Indeed, according to Fig. 1.a, $\langle C \perp_{\mathcal{G}^*} D | \mathbf{Z} \rangle$ for any $\mathbf{Z} \subseteq \mathbf{X}_O \setminus \{C, D\}$ equal to \emptyset , $\{A\}$ or $\{B\}$. Unfortunately, for the same reason that Types 1, 2 and 3 triangles encode the same d -separation properties, the orientations of the arcs of Triangle (D, B, C) can be reversed (provided they do not induce directed cycles). As a consequence, in the learnt graph \mathcal{G} , node D may be a child of B rather than its parent. At first sight, it is difficult to discriminate between the true children of B in \mathcal{G}^* and its true parents in which the arcs of Triangle (D, B, C) have been reversed. However, note that if D were a true child of B in \mathcal{G}^* , $\langle C \perp_{\mathcal{G}^*} D | \mathbf{Z} \rangle$ would hold for \mathbf{Z} only equal to \emptyset or $\{B\}$ (see Fig. 1.a). As a consequence, only the true parents D of B in \mathcal{G} are such that $\langle C \perp_{\mathcal{G}^*} D | \mathbf{Z} \rangle$ given some set $\mathbf{Z} \subseteq \mathbf{X}_O \setminus \{C, D\}$ containing node A . So Type 3 triangles are considered as latent only if they satisfy both this property and Rule 2. Overall, this results in Algorithm 1.

Remark that, as mentioned previously, on Line 12, Algorithm 1 is allowed to remove Arc $A \rightarrow B$ because, when this arc truly exists in \mathcal{G}^* (see Fig. 2.d), based on Dataset \mathcal{D} , it is impossible for any learning algorithm to distinguish between \mathcal{G}^* and Fig. 2.e. In such a case, our algorithm deliberately chooses to return the structure of Fig. 2.e in order to enforce some Occam razor and to avoid requiring some expert knowledge to select the right structure.

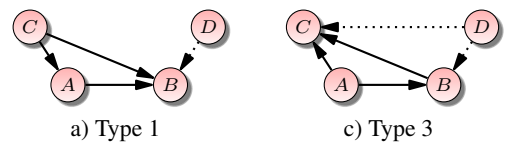


Figure 4: Arcs learnt in the vicinity of latent triangles.

Algorithm 1: Learning with confounders.

Input: Dataset \mathcal{D}
Output: The CPDAG of the learnt CBN

- 1 $\mathcal{G} \leftarrow$ DAG learnt from \mathcal{D} by a score-based algorithm
- 2 $\mathbf{T} \leftarrow$ the triangles of \mathcal{G} satisfying Rule 2
- // Get the latent triangles
- 3 $\mathbf{T}_1 \leftarrow \emptyset$ // latent triangles of type 1
- 4 $\mathbf{T}_3 \leftarrow \emptyset$ // latent triangles of type 3
- 5 **foreach** triangle $T = (A, B, C)$ in \mathbf{T} **do**
- 6 **if** T is of Type 1 and $|\text{Pa}_{\mathcal{G}}(B)| \geq 3$ **then**
- 7 $\mathbf{T}_1 \leftarrow \mathbf{T}_1 \cup T$
- 8 **else if** T is of Type 3 and there exists
- $D \in (\text{Pa}_{\mathcal{G}}(B) \setminus \{A\}) \cup (\text{Ch}_{\mathcal{G}}(B) \setminus \{C\})$ such that there
- exists $\mathbf{Z} \subseteq \mathbf{X}_O \setminus \{C, D\}$ such that $A \in \mathbf{Z}$ and
- $D \perp\!\!\!\perp_{\mathcal{P}(\mathbf{Z})} C$ **then**
- 9 $\mathbf{T}_3 \leftarrow \mathbf{T}_3 \cup T$
- // Recreate the latent variables
- 10 **foreach** triangle $T = (A, B, C)$ in $\mathbf{T}_1 \cup \mathbf{T}_3$ **do**
- 11 Add a new node L (confounder) to \mathcal{G}
- 12 Remove from \mathcal{G} Arc $A \rightarrow B$
- 13 Remove from \mathcal{G} the arc between B and C
- 14 Add arcs $L \rightarrow A$ and $L \rightarrow B$ to \mathcal{G}
- 15 $\mathcal{M} \leftarrow$ the CPDAG of \mathcal{G}
- 16 **return** CPDAG \mathcal{M}

Rule 2 and Algorithm 1 require the determination of some set $\mathbf{Z} \subseteq \mathbf{X}_O$ such that some pairs of nodes are conditionally independent given \mathbf{Z} . Below, we suggest two algorithms for this purpose. The first algorithm to determine Set \mathbf{Z} consists of exploiting the fact that, in I-maps, d -separation implies conditional independences. Hence, applying a d -separation analysis on \mathcal{G} using, e.g., van der Zander and Liškiewicz [28]’s algorithm, it is possible to get some d -separating set \mathbf{Z} and, consequently, a set inducing a conditional independence. The following proposition justifies that this approach can be used⁴:

Proposition 4. *Let \mathcal{D}^* be a dataset generated by some distribution P^* over \mathbf{X} for which there exists a perfect map $\mathcal{G}^* = (\mathbf{X}, \mathcal{E})$, and let \mathcal{D} be the projection of \mathcal{D}^* over \mathbf{X}_O . Then, as $|\mathcal{D}| \rightarrow \infty$, every DAG \mathcal{G} maximizing the BIC score over \mathcal{D} is a minimal I-map.*

However, when the database is not “too” large and Graph \mathcal{G} is not highly trustworthy, another option is to exploit Algorithm 2 which adds iteratively to \mathbf{Z} the variable X that allows to reduce the most the dependence between the pair of nodes U, V until an independence between U and V is inferred or no independence can be proven. In essence, this is the approach followed by MIIC [30], except that MIIC estimates dependences through an information theoretic criterion whereas we exploit the BIC score:

Definition 4. *For every pair of variables U, V and every set of variables \mathbf{Z} , let $f_{BIC}(U, V | \mathbf{Z})$ be defined as:*

$$f_{BIC}(U, V | \mathbf{Z}) = 2 \times \left(S(U|V, \mathbf{Z}) - S(U|\mathbf{Z}) + \frac{1}{2} \log(|\mathcal{D}|) \delta \right) \quad (5)$$

where $\delta = (|\Omega_U| - 1) \times (|\Omega_V| - 1) \times |\Omega_{\mathbf{Z}}|$ and Ω_U (resp. $\Omega_V, \Omega_{\mathbf{Z}}$) is the domain of variable U (resp. V, \mathbf{Z}), and $S(\cdot | \cdot)$ is the BIC score.

The following proposition justifies Algorithm 2:

⁴ The asymptotic consistency of the BIC score was already known in other cases [1, 9].

Algorithm 2: Finding a set \mathbf{Z} s.t. $U \perp\!\!\!\perp V | \mathbf{Z}$

Input: nodes U, V , Dataset \mathcal{D} , max size h of \mathbf{Z} , risk level α , sets \mathbf{C} and \mathbf{F} of compulsory and forbidden variables, i.e., \mathbf{Z} must satisfy $\mathbf{Z} \supseteq \mathbf{C}$ and $\mathbf{Z} \cap \mathbf{F} = \emptyset$
Output: A set \mathbf{Z} s.t. $U \perp\!\!\!\perp V | \mathbf{Z}$ if such set is found, else False

- 1 $\mathbf{Z} \leftarrow \mathbf{C}; \mathbf{F} \leftarrow \mathbf{F} \cup \{U, V\}$
- 2 $\delta \leftarrow (|\Omega_U| - 1) \times (|\Omega_V| - 1) \prod_{X \in \mathbf{C}} |\Omega_X|$
- 3 **if** $|\mathbf{Z}| > h$ **then return** False;
- 4 **if** $f_{BIC}(U, V | \mathbf{Z}) < \chi_{\delta}^2(\alpha)$ **then return** \mathbf{Z} ;
- 5 **while** $|\mathbf{Z}| < h$ **do**
- 6 $X = \text{argmin}\{f_{BIC}(U, V | \mathbf{Z} \cup \{Y\}) : Y \in \mathbf{X}_O \setminus (\mathbf{Z} \cup \mathbf{F})\}$
- 7 $\mathbf{Z} \leftarrow \mathbf{Z} \cup \{X\}$
- 8 $\delta \leftarrow \delta \times |\Omega_X|$
- 9 **if** $f_{BIC}(U, V | \mathbf{Z}) < \chi_{\delta}^2(\alpha)$ **then return** \mathbf{Z} ;
- 10 **return** False

Proposition 5. *If U and V are independent given a set \mathbf{Z} , the formula of Eq. (5) follows a χ^2 distribution of δ degrees of freedom. So, given a risk level α , U and V are judged independent if the value of Eq. (5) is lower than the critical value $\chi_{\delta}^2(\alpha)$ of the χ^2 distribution.*

To conclude this section, we provide below the time complexity of Algorithm 1, assuming (as we did in our experiments) that the algorithm used for determining the conditioning sets \mathbf{Z} required in Rule 2 and Algorithm 1 is Algorithm 2:

Proposition 6. *Assume that the existence of d -separating sets \mathbf{Z} is checked with Algorithm 2 with h the maximal size allowed for \mathbf{Z} and f_{BIC} defined as Eq. (5). Let n and m denote the number of nodes and arcs of \mathcal{G} as defined on Line 1 respectively. Let k be the maximum number of parents and children of the nodes in \mathcal{G} . Then the time complexity of Algorithm 1 over dataset \mathcal{D} is $O(n^2 k^3 h |\mathcal{D}| + m \log n)$.*

4 Experiments

In this section, some experiments on classical benchmark CBNs (child ($|\mathbf{X}_O| = 20$), water ($|\mathbf{X}_O| = 32$), insurance ($|\mathbf{X}_O| = 27$), alarm ($|\mathbf{X}_O| = 37$), barley ($|\mathbf{X}_O| = 48$)) from the BNLearn Bayes net repository⁵ are performed to highlight the effectiveness of our algorithm to find latent confounders and to recover CBN structures.

For each experiment, a CBN is selected, and some new (latent) variables L_i are added to it. To make them confounders of a semi-Markovian causal model, for each L_i , two nodes of \mathbf{X}_O are randomly chosen to become L_i ’s children. To fit the propositions of the paper, Line 1 of Algorithm 1 is performed using the CPBayes exact score-based learning algorithm [26]. For this purpose, Datasets \mathcal{D} need to be converted into so-called *instances* that are passed as input to CPBayes. These contain all the possible nodes’ sets that CPBayes will consider as potential parent sets. So, to control the combinatorial explosion it has to face, CPBayes requires limiting the number of possible parents of the nodes. In the experiments, we set this limit to 4 because i) no node of \mathbf{X}_O had more than 4 parents in the original CBN (the one without confounders); and ii) this enabled to control the amount of computations performed by CPBayes (see [26] for more details). As a consequence, since the score-based algorithm may add 2 additional parents (A and C) to some L_i ’s children (B), as shown in Fig. 1.b, all the L_i ’s children are selected randomly but with the constraint that they have 1 or 2 parents in \mathbf{X}_O . This upper bound

⁵ <https://www.bnlearn.com/bnrepository>

CBN	\mathcal{D}	Algorithm 1					MIIC					FCI					
		ok	-ok	prec.	recall	F1	time	ok	-ok	prec.	recall	F1	ok	-ok	prec.	recall	F1
child	5000	0.50	0.06	0.89	0.25	0.39	0.014	1.40	0.74	0.65	0.70	0.68	1.76	3.96	0.31	0.88	0.46
	10000	0.76	0.18	0.81	0.38	0.52	0.028	1.58	0.62	0.72	0.79	0.75	1.86	2.92	0.39	0.93	0.55
	20000	1.10	0.12	0.90	0.55	0.68	0.050	1.34	0.80	0.63	0.67	0.65	1.74	2.12	0.45	0.87	0.59
	50000	1.42	0.14	0.91	0.71	0.80	0.103	1.40	0.68	0.67	0.70	0.69	1.74	1.08	0.62	0.87	0.72
	100000	1.44	0.14	0.91	0.72	0.80	0.190	1.46	0.56	0.72	0.73	0.73	1.72	0.68	0.72	0.86	0.78
water	5000	0.16	1.56	0.09	0.08	0.09	0.017	0.34	2.76	0.11	0.17	0.13	0.34	8.26	0.04	0.17	0.06
	10000	0.44	0.04	0.92	0.22	0.35	0.043	1.24	1.68	0.42	0.62	0.50	1.54	5.40	0.22	0.77	0.34
	20000	0.80	0.22	0.78	0.40	0.53	0.104	1.40	1.88	0.43	0.70	0.53	1.60	6.04	0.21	0.80	0.33
	50000	1.16	0.60	0.66	0.58	0.62	0.132	1.40	1.92	0.42	0.70	0.53	1.56	7.86	0.17	0.78	0.27
	100000	1.22	1.04	0.54	0.61	0.57	0.248	1.44	2.78	0.34	0.72	0.46	1.52	8.32	0.15	0.76	0.26
insu- rance	5000	0.20	0.20	0.50	0.10	0.17	0.042	1.62	4.04	0.29	0.81	0.42	1.88	8.86	0.18	0.94	0.30
	10000	0.30	0.28	0.52	0.15	0.23	0.079	1.48	3.32	0.31	0.74	0.44	1.96	8.78	0.18	0.98	0.31
	20000	0.62	0.30	0.67	0.31	0.42	0.172	1.66	3.88	0.30	0.83	0.44	1.94	8.44	0.19	0.97	0.31
	50000	1.16	0.54	0.68	0.58	0.63	0.373	1.78	3.48	0.34	0.89	0.49	1.90	8.66	0.18	0.95	0.30
	100000	1.32	0.72	0.65	0.66	0.65	0.791	1.76	3.00	0.37	0.88	0.52	1.76	8.20	0.18	0.88	0.29
alarm	5000	0.36	0.40	0.47	0.18	0.26	0.058	1.24	1.98	0.46	0.62	0.53	1.48	4.74	0.24	0.74	0.36
	10000	0.86	0.58	0.60	0.43	0.50	0.119	1.50	0.98	0.60	0.75	0.67	1.56	4.14	0.27	0.78	0.41
	20000	1.12	0.66	0.63	0.56	0.59	0.180	1.50	0.52	0.74	0.75	0.75	1.72	3.42	0.33	0.86	0.48
	50000	1.36	1.16	0.54	0.68	0.60	0.385	1.64	1.04	0.61	0.82	0.70	1.68	2.92	0.37	0.84	0.51
	100000	1.44	1.18	0.55	0.72	0.62	0.744	1.62	0.76	0.68	0.81	0.74	1.70	2.42	0.41	0.85	0.56
barley	5000	0.02	0.00	1.00	0.01	0.02	0.013	0.60	3.14	0.16	0.30	0.21	1.58	20.70	0.07	0.79	0.13
	10000	0.08	0.00	1.00	0.04	0.08	0.032	0.74	2.30	0.24	0.37	0.29	1.78	19.72	0.08	0.89	0.15
	20000	0.36	0.00	1.00	0.18	0.31	0.076	1.02	1.84	0.36	0.51	0.42	1.86	16.56	0.10	0.93	0.18
	50000	0.74	0.00	1.00	0.37	0.54	0.229	1.34	3.72	0.26	0.67	0.38	1.86	14.86	0.11	0.93	0.20
	100000	0.96	0.08	0.92	0.48	0.63	0.511	1.36	2.96	0.31	0.68	0.43	1.84	13.70	0.12	0.92	0.21

Table 1: Confounders found for different dataset sizes and CBNs with 2 Boolean confounders.

constraint is only due to our use of CPBayes, not to Algorithm 1. But the lower bound is due to Proposition 2.

To discover that some nodes A and B are children of some confounder L_i , all the learning algorithms rely in some way or another on the fact that A and B are conditionally dependent given any set \mathbf{Z} . This imposes some restrictions on the way the conditional probability distributions (CPD) of L_i and its children should be generated. Actually, assume that they are uniformly randomly generated. Then the cells of the joint distribution P of A , B and their parents is a sample generated from a uniform distribution. Testing the conditional (in)dependence of A and B given some sets \mathbf{Z} strictly included in A and B 's parents amounts to marginalize out some variables from P or, equivalently, to sum some values of P . The sum of 2 independent variables uniformly distributed follows a triangular distribution and, by the central limit theorem, the sum of more than 2 variables tends to a variable normally distributed. As such, the values of the marginals of P have much more chances to be located on the mode of the distribution than on the tails. In other words, the cells of the marginals of P tend to have more or less the same values, which makes A and B appear to be independent, and no learning algorithm can determine that they are the children of a confounder. This is the reason why the CPDs of A , B and L_i need to be generated differently.

In our experiments, the CPD of L_i is set to a uniform distribution in order to maximize the chances of A and B to be dependent. For A (resp. B), for each value of its parents, the CPD of A (resp. B) is set to a mixture of a Dirichlet distribution whose hyperparameters α_i are all set to 4 and a Dirac distribution. The weight of the latter is selected randomly between $2/3$ and $5/6$. Such mixtures tend experimentally to limit the effect of the central limit theorem but, of course, do not discard it completely. So, to check whether A and B have some chance to be identified as dependent, we test whether the values of their mutual information and their conditional mutual information given their parents are higher than some thresholds (these are some extreme cases for the \mathbf{Z} sets mentioned in the preceding paragraph). If this is the case, the CPDs of A and B are judged admissible for the experiments. To make them realistic, the thresholds are defined as the averages of the mutual information and condition mutual infor-

mation respectively of all the pairs of nodes with a common parent in the original CBN. The use of these information-theoretic criteria has been made to favor algorithms like MIIC over our algorithm.

For each CBN with confounders created as defined above, a dataset \mathcal{D}^* is randomly generated using the pyAgrum 1.13.0 library [7] and Dataset \mathcal{D} which is given as input of the learning algorithms is the projection of \mathcal{D}^* over \mathbf{X}_O . Algorithm 2 is exploited for independence testing and its risk level α and Size h are set to 0.05 and 7 respectively⁶. In the experiments, we compare 3 learning algorithms: Algorithm 1, MIIC [30] and FCI [21]. For MIIC, we use the pyAgrum's implementation with the NML correction to be more accurate. For FCI, we use the python causal-learn 0.1.3.8 package [32]. All the tables below display averages of the results over 50 CBN/datasets. All the experiments are executed on an Intel Xeon Gold 5218 CPU with 128GB of RAM.

In Table 1, to every original CBN, 2 confounders have been added whose domain sizes are equal to 2. The table compares the performance of Algorithm 1, MIIC and FCI for different CBNs with different dataset sizes. Columns ok and -ok contain the number of correctly and wrongly identified confounders respectively. Column "prec." displays the precision metrics, i.e., it is equal to ok / (ok + -ok). Column "recall" is the usual recall metrics, i.e., it is equal to ok / the number of confounders L_i added to the original CBN. The F1 score is defined as $2 \times (\text{precision} \times \text{recall}) / (\text{precision} + \text{recall})$. Column "time" reports the average computation times in seconds of Lines 2 to 16 of Algorithm 1 (finding the confounders). These lines increase only marginally the structure learning computation times.

FCI finds most of the latent confounders. This is the reason why, in Table 1, it is the best in terms of *recall*. Unfortunately, it also misidentifies numerous variables as confounder's children. This is the reason why its precision and F1 score are, by far, never the best. Here, we should emphasize that we identify confounders with \leftrightarrow connections, that is, we do not take into account \circ labels since those express an uncertainty about the existence of arrow heads. Converting every \rightarrow into \leftrightarrow results in adding numerous false positive, which would de-

⁶ Sets \mathbf{Z} may include other nodes than just the sets of parents of U or V . Hence, for robustness, we allowed to almost double their maximal size h .

CBN	$ \mathcal{D} $	Algorithm 1					MIIC					FCI				
		ok	miss	rev.	type	xs	ok	miss	rev.	type	xs	ok	miss	rev.	type	xs
child	5000	22.46	3.08	1.02	2.44	2.54	19.46	2.00	3.18	4.36	3.42	15.00	4.96	0.22	8.82	8.00
	10000	23.10	2.52	1.52	1.86	3.12	20.72	1.18	3.28	3.82	3.42	15.64	3.40	0.06	9.90	6.00
	20000	22.88	1.84	2.22	2.06	3.62	19.94	1.44	2.84	4.78	3.82	16.70	2.60	0.00	9.70	4.44
	50000	22.98	1.22	2.84	1.96	4.34	20.36	1.30	2.98	4.36	3.74	20.80	1.54	0.00	6.66	2.54
	100000	23.20	1.14	2.88	1.78	4.50	21.28	1.14	3.04	3.54	3.72	22.38	1.22	0.00	5.40	1.88
water	5000	16.72	40.18	4.72	8.38	4.60	15.48	40.20	7.26	7.06	9.38	13.46	45.54	1.38	9.62	11.50
	10000	19.00	36.98	7.58	6.44	5.96	17.82	37.78	8.04	6.36	9.40	17.90	43.02	1.02	8.06	12.82
	20000	21.12	36.64	6.82	5.42	8.72	21.84	38.10	4.78	5.28	11.36	17.76	43.76	0.52	7.96	16.88
	50000	26.22	32.48	7.20	4.10	7.02	23.76	34.70	6.12	5.42	10.58	25.12	38.66	0.76	5.46	16.42
	100000	29.94	29.42	7.10	3.54	7.06	27.44	32.32	5.34	4.90	12.54	26.80	37.68	0.52	5.00	17.26
insurance	5000	32.38	14.44	2.46	6.72	3.82	29.20	12.70	3.60	10.50	12.44	23.90	21.60	0.46	10.04	18.06
	10000	34.68	12.22	2.38	6.72	4.06	29.86	11.70	3.52	10.92	11.46	25.76	18.64	0.30	11.30	17.72
	20000	38.76	9.20	3.34	4.70	5.04	30.42	10.00	3.74	11.84	13.12	27.98	16.18	0.14	11.70	17.08
	50000	41.08	7.58	4.42	2.92	6.42	31.32	8.34	4.00	12.34	12.94	29.42	13.92	0.10	12.56	17.70
	100000	40.34	7.08	4.94	3.64	7.48	31.46	7.88	3.88	12.78	13.40	31.36	12.64	0.12	11.88	16.96
alarm	5000	38.10	6.42	3.90	1.58	5.08	40.04	5.54	3.10	1.32	7.72	37.34	10.36	0.58	1.72	10.40
	10000	39.08	4.52	4.96	1.44	5.88	40.92	4.46	3.30	1.32	6.72	39.48	8.88	0.46	1.18	9.22
	20000	40.64	3.08	5.02	1.26	5.82	42.48	3.54	3.32	0.66	5.92	42.90	6.06	0.18	0.86	7.60
	50000	40.28	2.62	5.86	1.24	7.46	42.46	3.02	3.60	0.92	8.16	43.44	5.48	0.18	0.90	6.58
	100000	40.72	1.84	6.02	1.42	7.72	43.04	2.44	3.66	0.86	7.76	44.66	4.18	0.10	1.06	5.60
barley	5000	41.46	34.66	3.02	8.86	6.32	51.12	25.14	4.32	7.42	13.74	42.48	38.30	2.08	5.14	42.46
	10000	46.30	29.10	2.82	9.78	5.40	56.10	21.52	4.44	5.94	13.34	47.48	33.70	1.38	5.44	40.72
	20000	52.08	22.70	3.74	9.48	4.64	60.26	17.90	4.80	5.04	13.44	53.72	27.32	1.68	5.28	34.70
	50000	57.74	17.96	4.28	8.02	4.54	67.24	12.96	4.42	3.38	20.72	59.74	21.26	1.34	5.66	31.02
	100000	62.52	14.80	5.00	5.68	4.48	69.72	12.16	3.96	2.16	21.76	62.14	19.16	1.02	5.68	29.30

Table 2: Comparisons of the learnt CPDAGs with those of the CBNs (with confounders) that generated the datasets.

crease significantly the quality of the solutions found by FCI.

MIIC identifies fewer confounders but it also makes much fewer mistakes, which makes it better in terms of F1 score. Algo. 1 makes even fewer mistakes and this is the reason why its precision is almost always the best of all the algorithms. Yet, it is somewhat cautious and tends to miss some confounders, which explains why its *recall* is not the best. However, the larger the size of the dataset, the higher the number of confounders correctly identified by Algorithm 1. This can also be observed in terms of F1 score: for small datasets, MIIC outperforms Algorithm 1 but this is the converse when $|\mathcal{D}|$ increases. This phenomenon illustrates empirically Proposition 1.

Table 2 reports how the CPDAGs learnt by Algorithm 1, MIIC and FCI compare with those of the CBNs (with their confounders) that were used to generate the datasets. Columns “ok” (resp. “miss”) indicate the number of arcs and edges that were learnt correctly (resp. that existed in the generating CBN but for which no arc nor edge was learnt). As can be observed, Algorithm 1 and MIIC are the best for these metrics and their results are quite comparable. Of course, for these metrics, the larger the dataset, the better the quality of the learnt CPDAGs. Column “rev.” displays the number of arcs in the CPDAG of the generating CBN that were learnt in the opposite direction, i.e., the direction of the causality is incorrectly learnt. For this metrics, FCI always outperforms the other algorithms. Note, however, that the number of reversed arcs is always very small for all the CBNs and all dataset sizes. Column “type” refers to the number of arcs (resp. edges) that were learnt as edges (resp. arcs), i.e., their types (directed, undirected) are incorrect. For this metrics, Algorithm 1 and MIIC usually outperform FCI and, in general, when Algorithm 1 outperforms MIIC, the difference is bigger than when this is the converse. Finally, Column “xs” reports the number of arcs or edges that belong to the learnt CPDAG but whose extremal nodes are linked neither by an arc nor by an edge in the generating CBN. Here, Algorithm 1 significantly outperforms both MIIC and FCI. This means that Algorithm 1 is less prone to learn spurious direct causes. Overall, empirically, Algorithm 1 is very competitive and often produces CPDAGs closer to those of the original CBNs than the other two methods

5 Conclusion and Perspectives

In this paper, we have introduced the first score-based CBN structure learning algorithm for discrete variables that searches only the space of DAGs, exploits only observational data and, yet, is capable of identifying some latent confounders. It has been justified mathematically, notably through Proposition 1. In addition, theoretically, it is asymptotically guaranteed to produce an I-map. Experiments highlighted its effectiveness, especially for large datasets. Notably, both in terms of the CPDAGs and the latent confounders found, the results of this algorithm may be judged as very competitive compared to those of its constraint-based competitors like MIIC or FCI.

For future works, to be more scalable, we plan to substitute the use of the CPBayes on Line 1 of Algorithm 1 by a faster approximate algorithm like greedy hill climbing (GHC). Usually, GHC-like methods make more mistakes in the directions of the causal arcs learned than CPBayes. So, to compensate for this issue, the rules used in Lines 6 and 8 may certainly have to be improved. Notably, in Algorithm 1, we did not take into account Type 2 triangles (see Figure 3.b) because, empirically, they were very seldom encountered in the experiments. However, with GHC-like algorithms, this may not be the case anymore and they should be taken into account.

Perhaps a more immediate improvement could be made by observing that, whenever Type 3 triangles are found, their $A \rightarrow C$ connection is in the wrong direction (see Figure 3.b). Therefore, to produce better CPDAGs, Algorithm 1 should reverse this arc and relearn the neighborhood of node C . In addition, as shown in Propositions 2 and 3, some structures are indistinguishable from the observational data point of view and, among all the structures of Fig. 2, Algorithm 1 makes the decision to select only those of Fig. 2.c and 2.e. So, in the same spirit as PAGs, the output of Algorithm 1 could be improved to express the uncertainty about which of these structures should be selected. Note that, in this case, PAG’s \circ labels are not sufficient since the uncertainty not only concerns the location of arrow heads but also the very existence of some arcs (like $C \rightarrow B$ of Fig. 2.e) for which no independence test can detect that they can be dispensed with.

References

- [1] R. R. Bouckaert. Probabilistic network construction using the minimum description length principle. In *Proc. of the European conference on symbolic and quantitative approaches to reasoning and uncertainty (ECSQARU'93)*, pages 41–48, 1993.
- [2] D. Chickering. A transformational characterization of equivalent Bayesian network structures. In *Proc. of UAI*, pages 87–98, 1995.
- [3] M. Chickering. Optimal structure identification with greedy search. *Journal of Machine Learning Research*, 3:507–554, 2002.
- [4] D. Colombo and M. Maathuis. Order-independent constraint-based causal structure learning. *Journal of Machine Learning Research*, 15: 3921–3962, 2014.
- [5] D. Colombo, M. Maathuis, M. Kalisch, and T. Richardson. Learning high-dimensional directed acyclic graphs with latent and selection variables. *The Annals of Statistics*, 40(1):294–321, 2012.
- [6] G. Cooper and E. Herskovits. A Bayesian method for the induction of probabilistic networks from data. *Machine Learning*, 9(4):309–347, 1992.
- [7] G. Ducamp, C. Gonzales, and P.-H. Wuillemin. aGrUM/pyAgrum: a toolbox to build models and algorithms for probabilistic graphical models in python. In *Proc. of the International Conference on Probabilistic Graphical Models (PGM'20)*, pages 609–612, 2020.
- [8] D. Heckerman, D. Geiger, and D. Chickering. Learning Bayesian networks: The combination of knowledge and statistical data. *Machine Learning*, 20:197–243, 1995.
- [9] D. Koller and N. Friedman. *Probabilistic Graphical Models: Principles and Techniques*. MIT Press, 2009.
- [10] J. Lemeire, S. Meganck, F. Cartella, and T. Liu. Conservative independence-based causal structure learning in absence of adjacency faithfulness. *International Journal of Approximate Reasoning*, 53(9): 1305–1325, 2012.
- [11] A. Mabrouk, C. Gonzales, K. Jabet-Chevalier, and E. Chojnaki. An efficient Bayesian network structure learning algorithm in the presence of deterministic relations. In *Proc. of the European Conference on Artificial Intelligence (ECAI'14)*, pages 567–572, 2014.
- [12] C. Meek. Causal inference and causal explanation with background knowledge. In *Proc. of the Conference on Uncertainty in Artificial Intelligence (UAI'95)*, pages 403–410, 1995.
- [13] J. Ogarrio, P. Spirtes, and J. Ramsey. A hybrid causal search algorithm for latent variable models. In *Proc. of International Conference on Probabilistic Graphical Models (PGM'16)*, pages 368–379, 2016.
- [14] J. Pearl. *Probabilistic Reasoning in Intelligent Systems: Networks of Plausible Inference*. Morgan Kaufman, 1988.
- [15] J. Pearl. *Causality*. Cambridge University Press, 2nd edition, 2009.
- [16] J. Ramsey, P. Spirtes, and J. Zhang. Adjacency-faithfulness and conservative causal inference. In *Proc. of the Conference on Uncertainty in Artificial Intelligence (UAI'06)*, pages 401–408, 2006.
- [17] T. Richardson and P. Spirtes. Scoring ancestral graph models. Technical Report CMU-PHIL-98, Carnegie Mellon, 1998.
- [18] T. Richardson and P. Spirtes. Ancestral graph markov models. *Annals of Statistics*, 30(4):962–1030, 2002.
- [19] G. Schwarz. Estimating the dimension of a model. *Annals of Statistics*, 6:461–464, 1978.
- [20] P. Spirtes and C. Glymour. An algorithm for fast recovery of sparse causal graphs. *Social Science Computer Review*, 9(1):62–72, 1991.
- [21] P. Spirtes, C. Glymour, and R. Scheines. *Causation, Prediction, and Search*. MIT press, 2nd edition, 2000.
- [22] J. Tian and J. Pearl. On the identification of causal effects. Technical Report R-290-L, UCLA C.S. Lab, 2002.
- [23] S. Triantafillou and I. Tsamardinos. Score based vs constraint based causal learning in the presence of confounders. In *Proc. of the "Causation: Foundation to Application" Workshop, Uncertainty in Artificial Intelligence*, 2016.
- [24] F. Trösser, S. de Givry, and G. Katsirelos. "structured set variable domains in Bayesian network structure learning. In *Proc. of Principles and Practice of Constraint Programming (CP'22)*, pages 37:1–37:9, 2022.
- [25] I. Tsamardinos, C. Aliferis, and S. Statnikov. Algorithms for large scale Markov blanket discovery. In *Proc. of the international FLAIRS conference (FLAIRS'03)*, pages 376–381, 2003.
- [26] P. van Beek and H.-F. Hoffmann. Machine learning of Bayesian networks using constraint programming. In *Proc. of Principles and Practice of Constraint Programming (CP'15)*, pages 429–445, 2015.
- [27] P. van Beek and C. Lee. An experimental analysis of anytime algorithms for Bayesian network structure learning. *Proceedings of Machine Learning Research*, 73:69–80, 2017.
- [28] B. van der Zander and M. Liškiewicz. Finding minimal d-separators in linear time and applications. In *Proc. of the Conference on Uncertainty in Artificial Intelligence Conference (UAI'20)*, pages 637–647, 2020.
- [29] T. Verma and J. Pearl. Equivalence and synthesis of causal models. In *Proc. of the Conference on Uncertainty in Artificial Intelligence (UAI'90)*, pages 220–227, 1990.
- [30] L. Verny, N. Sella, S. Affeldt, P. Singh, and H. Isambert. Learning causal networks with latent variables from multivariate information in genomic data. *PLOS Computational Biology*, 2017.
- [31] J. Zhang. On the completeness of orientation rules for causal discovery in the presence of latent confounders and selection bias. *Artificial Intelligence*, 172(16):1873–1896, 2008.
- [32] Y. Zheng, B. Huang, W. Chen, J. Ramsey, M. Gong, R. Cai, S. Shimizu, P. Spirtes, and K. Zhang. Causal-learn: causal discovery in python. *arXiv preprint arXiv:2307.16405*, 2023.

Supplementary Material

A Proofs

Below are the proofs of all the propositions of the paper.

Lemma 1. Let \mathbf{X}_O and \mathbf{X}_H be two disjoint sets of random variables and let $\mathbf{X} = \mathbf{X}_O \cup \mathbf{X}_H$. Let \mathcal{D}^* be a dataset generated by some distribution P^* over \mathbf{X} for which there exists a perfect map $\mathcal{G}^* = (\mathbf{X}, \mathcal{E})$, and let \mathcal{D} be the projection of \mathcal{D}^* over \mathbf{X}_O , i.e., the dataset resulting from the removal from \mathcal{D}^* of all the values of the variables of \mathbf{X}_H . Let \mathcal{G} be a DAG maximizing the BIC score over \mathcal{D} . Then, as $|\mathcal{D}| \rightarrow \infty$, if, in Graph \mathcal{G} , there is no arc between a pair of nodes (A, B) and no directed path⁷ from B to A , then $A \perp_{P^*} B | \mathbf{Pa}_{\mathcal{G}}(B)$.

Proof of Lemma 1. As there is no directed path from B to A in \mathcal{G} , adding $A \rightarrow B$ cannot create a directed cycle, hence this would produce a new DAG. If \mathcal{G} does not contain this arc, this therefore means that the BIC score $S(B | \mathbf{Pa}_{\mathcal{G}}(B) \cup \{A\})$ is lower than or equal to $S(B | \mathbf{Pa}_{\mathcal{G}}(B))$. \mathcal{D} is the projection of \mathcal{D}^* over \mathbf{X}_O , so the distribution P which generated \mathcal{D} is the projection of P^* over \mathbf{X}_O , hence, for any $\mathbf{Z}, \mathbf{W} \subseteq \mathbf{X}_O$, $P(\mathbf{Z} | \mathbf{W}) = P^*(\mathbf{Z} | \mathbf{W})$. As a consequence, as $|\mathcal{D}| \rightarrow \infty$, the BIC score can be expressed in terms of mutual information (\mathbf{I}_{P^*}) and entropy (\mathbf{H}_{P^*}) over P^* [9, p792]:

$$S(B | \mathbf{Pa}_{\mathcal{G}}(B) \cup \{A\}) \rightarrow |\mathcal{D}| \times [\mathbf{I}_{P^*}(B; \mathbf{Pa}_{\mathcal{G}}(B) \cup \{A\}) - \mathbf{H}_{P^*}(B)] - \frac{\log |\mathcal{D}|}{2} \dim(B | \mathbf{Pa}_{\mathcal{G}}(B) \cup \{A\}),$$

where, for all Z, \mathbf{W} :

$$\dim(B | \mathbf{Pa}_{\mathcal{G}}(B) \cup \{A\}) = (|\Omega_B| - 1) \times |\Omega_A| \times \prod_{x \in \mathbf{Pa}_{\mathcal{G}}(B)} |\Omega_x|,$$

$$\mathbf{I}_{P^*}(Z; \mathbf{W}) = \sum_{z \in \Omega_Z} \sum_{\mathbf{w} \in \Omega_{\mathbf{W}}} P^*(z, \mathbf{w}) \log \left(\frac{P^*(z, \mathbf{w})}{P^*(z) P^*(\mathbf{w})} \right),$$

$$\mathbf{H}_{P^*}(Z) = \sum_{z \in \Omega_Z} P^*(z) \log(P^*(z)).$$

So, if α denotes the difference between the two scores, we have that:

$$\begin{aligned} \alpha &= S(B | \mathbf{Pa}_{\mathcal{G}}(B) \cup \{A\}) - S(B | \mathbf{Pa}_{\mathcal{G}}(B)) \\ &= |\mathcal{D}| \times [\mathbf{I}_{P^*}(B; \mathbf{Pa}_{\mathcal{G}}(B) \cup \{A\}) - \mathbf{I}_{P^*}(B; \mathbf{Pa}_{\mathcal{G}}(B))] \\ &\quad - \delta \log |\mathcal{D}| / 2, \end{aligned}$$

with $\delta = \dim(B | \mathbf{Pa}_{\mathcal{G}}(B) \cup \{A\}) - \dim(B | \mathbf{Pa}_{\mathcal{G}}(B))$. When $|\mathcal{D}| \rightarrow \infty$, $\log |\mathcal{D}|$ is infinitely smaller than $|\mathcal{D}|$. Hence $\alpha \leq 0$ if and only if $\mathbf{I}_{P^*}(B; \mathbf{Pa}_{\mathcal{G}}(B) \cup \{A\}) \leq \mathbf{I}_{P^*}(B; \mathbf{Pa}_{\mathcal{G}}(B))$. But, for every probability distribution Q and every X, Y, \mathbf{Z} , it always holds that $\mathbf{I}_Q(X; \mathbf{Z} \cup \{Y\}) \geq \mathbf{I}_Q(X; \mathbf{Z})$, with equality only if $X \perp_Q Y | \mathbf{Z}$. Hence $\alpha \leq 0$ if and only if $\mathbf{I}_{P^*}(B; \mathbf{Pa}_{\mathcal{G}}(B) \cup \{A\}) = \mathbf{I}_{P^*}(B; \mathbf{Pa}_{\mathcal{G}}(B))$. This implies that $A \perp_{P^*} B | \mathbf{Pa}_{\mathcal{G}}(B)$. ■

Corollary 1. Let \mathbf{X}_O and \mathbf{X}_H be two disjoint sets of random variables and let $\mathbf{X} = \mathbf{X}_O \cup \mathbf{X}_H$. Let \mathcal{D}^* be a dataset generated by some distribution P^* over \mathbf{X} for which there exists a perfect map $\mathcal{G}^* = (\mathbf{X}, \mathcal{E})$, and let \mathcal{D} be the projection of \mathcal{D}^* over \mathbf{X}_O . Let \mathcal{G} be a DAG maximizing the BIC score over \mathcal{D} . Then, as $|\mathcal{D}| \rightarrow \infty$, for any $A, B \in \mathbf{X}_O$, if \mathcal{G}^* contains Arc $A \rightarrow B$, then Graph \mathcal{G} contains either Arc $A \rightarrow B$ or $B \rightarrow A$.

Proof of Corollary 1. Assume that, for some pair $A, B \in \mathbf{X}_O$ such that there exists an arc between A and B in \mathcal{G}^* , Graph \mathcal{G} contains neither Arc $A \rightarrow B$ nor Arc $B \rightarrow A$. It is impossible that \mathcal{G} contains both a directed path from A to B and another one from B to A because the concatenation of these paths would be a directed cycle. Without loss of generality, assume that there exists no directed path from B to A in \mathcal{G} , then, by Lemma 1, $A \perp_{P^*} B | \mathbf{Pa}_{\mathcal{G}}(B)$. As \mathcal{G}^* is a perfect map, this implies that $\langle A \perp_{\mathcal{G}^*} B | \mathbf{Pa}_{\mathcal{G}}(\mathbf{B}) \rangle$, a contradiction since \mathcal{G}^* contains an arc between A and B . ■

Proof of Proposition 1. Let L be a variable in \mathbf{X}_H and let A, B be its children. Let \mathcal{G} be a graph maximizing the BIC score over \mathcal{D} . First, let us prove that there must exist an arc between A and B in \mathcal{G} . Assume the contrary. It is impossible that there exists both a directed path \mathcal{C}_{AB} from A to B in \mathcal{G} and a directed path \mathcal{C}_{BA} from B to A in \mathcal{G} because their concatenation would be a directed cycle, a contradiction since \mathcal{G} is a DAG. Without loss of generality, assume that there exists no directed path from B to A in \mathcal{G} . Then, as, by hypothesis, there exists no arc between A and B , by Lemma 1, $A \perp_{P^*} B | \mathbf{Pa}_{\mathcal{G}}(B)$. But this is impossible because, whatever the set $\mathbf{Z} \subseteq \mathbf{X}_O \setminus \{A, B\}$, Trail $\langle A, L, B \rangle$ is active given \mathbf{Z} in \mathcal{G}^* , so that $\langle A \not\perp_{\mathcal{G}^*} B | \mathbf{Pa}_{\mathcal{G}}(\mathbf{B}) \rangle$, which contradicts $A \perp_{P^*} B | \mathbf{Pa}_{\mathcal{G}}(B)$ since \mathcal{G}^* is a perfect map. So, there must exist an arc between A and B in \mathcal{G} . In the rest of the proof, without loss of generality, assume that it contains Arc $A \rightarrow B$.

Let $C \in \mathbf{Pa}_{\mathcal{G}^*}(A) \cap \mathbf{X}_O$. Such a C exists by the hypotheses at the beginning of the Proposition. By Corollary 1, \mathcal{G} contains an arc between A and C . As for an arc between B and C , assume that there exists none in \mathcal{G} . Note that Trail $\mathcal{C}_{CB} = \langle C, A, L, B \rangle$ is always active in \mathcal{G}^* given any $\mathbf{Z} \subseteq \mathbf{X}_O \setminus \{B, C\}$ that contains A . So $B \not\perp_{P^*} C | \mathbf{Z}$ since \mathcal{G}^* is a perfect map. Now, as shown at the beginning of the proof, there exists either i) no directed path from B to C in \mathcal{G} ; or ii) no directed path from C to B in \mathcal{G} . If Case i) obtains, by Lemma 1, $C \perp_{P^*} B | \mathbf{Pa}_{\mathcal{G}}(B)$, which is impossible since $A \in \mathbf{Pa}_{\mathcal{G}}(B)$ (according to the preceding paragraph), so that Trail \mathcal{C}_{CB} is active in \mathcal{G}^* given $\mathbf{Z} = \mathbf{Pa}_{\mathcal{G}}(B)$, a contradiction (since it is equivalent to $C \not\perp_{P^*} B | \mathbf{Pa}_{\mathcal{G}}(B)$). If Case ii) obtains (but not Case i)), then the arc added previously between A and C could not be $C \rightarrow A$ because, since Case i) does not obtain, there exists a directed path from B to C , hence also a directed path from A to C (since \mathcal{G} contains Arc $A \rightarrow B$). So Arc $C \rightarrow A$ would create a directed cycle. Hence, $A \in \mathbf{Pa}_{\mathcal{G}}(C)$. Now, by Lemma 1, $B \perp_{P^*} C | \mathbf{Pa}_{\mathcal{G}}(C)$, which is impossible since $\mathbf{Z} = \mathbf{Pa}_{\mathcal{G}}(C) \supseteq \{A\}$ would make Trail \mathcal{C}_{CB} active in \mathcal{G}^* , a contradiction. As a consequence, there must necessarily exist an arc between B and C in \mathcal{G} . So, overall, \mathcal{G} contains clique (A, B, C) . ■

Proof of Proposition 2. $\langle U \perp_{\mathcal{G}} V | \mathbf{W} \rangle$ is equivalent to $\langle U \perp_{\mathcal{G}} V | \mathbf{W} \rangle$ for all $U \in \mathbf{U}$ and $V \in \mathbf{V}$. So, we just need to prove that, for any $U, V \in \mathbf{X}_O$, $U \neq V$, $\langle U \perp_{\mathcal{G}} V | \mathbf{W} \rangle \iff \langle U \perp_{\mathcal{G}^*} V | \mathbf{W} \rangle$.

First, note that \mathcal{G}^* does not contain Arc $B \rightarrow A$, otherwise $\mathbf{Pa}_{\mathcal{G}^*}(A)$ would contain B . Adding Arc $A \rightarrow B$ cannot create a directed cycle in \mathcal{G}^* because A has only one parent, L , which cannot be involved in any cycle since it has no parent. Let $\mathbf{Desc}_{\mathcal{G}}(A)$ denote the set of descendants of A in \mathcal{G} , i.e., $\mathbf{Desc}_{\mathcal{G}}(A) = \{X : \text{there exists a directed path from } A \text{ to } X\}$. Note first that $\mathbf{Desc}_{\mathcal{G}}(A) = \mathbf{Desc}_{\mathcal{G}^*}(A) \cup \mathbf{Desc}_{\mathcal{G}^*}(B)$ and, for all $X \in \mathbf{X} \setminus \{A, L\}$, we have that $\mathbf{Desc}_{\mathcal{G}}(X) = \mathbf{Desc}_{\mathcal{G}^*}(X)$.

⁷ A directed path $\mathcal{C} = \langle X_1, \dots, X_k \rangle$ is a trail \mathcal{C} such that, for all $i \in \{1, \dots, k-1\}$, the graph contains Arc $X_i \rightarrow X_{i+1}$.

Now, consider any simple⁸ trail $C^* = \langle X_1 = U, \dots, X_k = V \rangle$ between U and V in \mathcal{G}^* . Assume it is blocked in \mathcal{G}^* . This is the case if and only if i) it contains a convergent connection at some node T such that neither T nor its descendants are in \mathbf{W} ; or ii) it contains a non-convergent connection at some node $T \in \mathbf{W}$.

Assume Trail C^* does not contain L , then it also exists in \mathcal{G} . Case i) cannot occur at $T = A$ because A has only one parent in \mathcal{G}^* or at $T = L$ because C^* does not contain L by hypothesis. Since all the other nodes in \mathcal{G}^* have the same set of descendants as their counterparts in \mathcal{G} , the convergent connections in C^* have therefore exactly the same status (blocked, active) in \mathcal{G} and \mathcal{G}^* . As for case ii), any non-convergent connection in C^* is the same in \mathcal{G} and \mathcal{G}^* and cannot involve L (by hypothesis). Hence, they have the same status in \mathcal{G} and \mathcal{G}^* . So C^* is blocked or active in both \mathcal{G} and \mathcal{G}^* .

Now, if C^* contains L , it includes the non-convergent connection $A \leftarrow L \rightarrow B$. Let \mathcal{C} be the trail of \mathcal{G} obtained from C^* by substituting $A \leftarrow L \rightarrow B$ by $A \rightarrow B$. For the same reasons as above, all the nodes different from A, L have the same connections in \mathcal{C} and C^* and the same set of descendants. Hence their status (blocked, active) are the same in \mathcal{C} and C^* . Node A cannot have a convergent connection in C^* because $\mathbf{Pa}_{\mathcal{G}^*}(A) = \{L\}$. In \mathcal{C} , its connection is also non-convergent since its child B in \mathcal{G} is its neighbor in \mathcal{C} . So, the connection at A is non-convergent and has the same status in both \mathcal{C} and C^* . Node L has a non-convergent connection in C^* but, as it is unobserved, it cannot belong to \mathbf{W} and cannot block the trail. So, removing it from C^* cannot change the status of the trail. Hence, overall, all the trails in \mathcal{G}^* can be mapped into a trail in \mathcal{G} with exactly the same status.

Conversely, let \mathcal{C} be a simple trail in \mathcal{G} . If this trail does not include Arc $A \rightarrow B$, then it also belongs to \mathcal{G}^* and the same reasoning as above shows that this trail has the same status in \mathcal{G} and \mathcal{G}^* .

If, on the other hand, \mathcal{C} contains Arc $A \rightarrow B$, then substituting it by $A \leftarrow L \rightarrow B$ results in a new trail C^* of \mathcal{G}^* . As above, all the nodes except A, B, L have the same status. In addition, L cannot block trail C^* and the connection at A is non-convergent in both \mathcal{C} and C^* (because it has at most one parent, L). If the connection at B is convergent in \mathcal{C} , it is also convergent in C^* , with its parent A substituted by L . If the connection at B in \mathcal{C} is non-convergent, this means that it is of the form $A \rightarrow B \rightarrow X$, and in C^* , its connection is $L \rightarrow B \rightarrow X$, also a non-convergent connection. Hence, overall, every trail of \mathcal{G} can be mapped into a trail of \mathcal{G}^* with the same status.

So, for all $U \in \mathbf{U}$ and $V \in \mathbf{V}$, we have that $\langle U \perp_{\mathcal{G}} V | \mathbf{W} \rangle \iff \langle U \perp_{\mathcal{G}^*} V | \mathbf{W} \rangle$. ■

Proof of Proposition 3. As for Proposition 2, we just need to prove that, for any $U, V \in \mathbf{X}_O$, $U \neq V$, $\langle U \perp_{\mathcal{G}} V | \mathbf{W} \rangle \iff \langle U \perp_{\mathcal{G}^*} V | \mathbf{W} \rangle$.

A simple trail $C^* = \langle X_1 = U, \dots, X_k = V \rangle$ between U and V is active in \mathcal{G}^* if and only if i) for all the nodes T with a convergent connection, either T or some of its descendants are in \mathbf{W} ; and ii) nodes T with non-convergent connections do not belong to \mathbf{W} . Note that, by definition of \mathcal{G} , if $\mathbf{Desc}_{\mathcal{G}}(X)$ denotes the set of descendants of Node X in \mathcal{G} , then $\mathbf{Desc}_{\mathcal{G}}(X) = \mathbf{Desc}_{\mathcal{G}^*}(X)$ for any $X \in \mathbf{X} \setminus \{L\}$. Let us first show that, if there exists an active trail in \mathcal{G}^* , then there also exists an active trail in \mathcal{G} .

Let C^* be an active trail of \mathcal{G}^* that does not contain L , then it also exists in \mathcal{G} and, since $\mathbf{Desc}_{\mathcal{G}}(X) = \mathbf{Desc}_{\mathcal{G}^*}(X)$ for all $X \in \mathbf{X} \setminus \{L\}$,

it is also an active trail of \mathcal{G} .

Assume now that Trail C^* contains L . Node L is equal neither to X_1 nor to X_k since U and V belong to \mathbf{X}_O . So, let $i \neq 1, k$ be the index such that, in Trail C^* , $X_i = L$. By definition of \mathcal{G}^* , it holds that $\{X_{i-1}, X_{i+1}\} = \{A, B\}$. Without loss of generality, assume below that $X_{i-1} = A$ and $X_{i+1} = B$ (if this is the converse, consider the reversed trail $\langle Y_1 = V, \dots, Y_k = U \rangle$, which has the same d -separation status as C^* , i.e., it is an active trail).

If $X_1 = A$, then A is the first node of Trail C^* . Let $\mathcal{C} = \langle X_1 = A, X_3 = B, X_4, \dots, X_k \rangle$. Then \mathcal{C} belongs to both \mathcal{G}^* and \mathcal{G} . In addition, the types of connection (convergent/non-convergent) of all the nodes X_3, \dots, X_{k-1} are the same in C^* and \mathcal{C} , and the sets of descendants of these nodes are the same in \mathcal{G}^* and \mathcal{G} . Finally, A and X_k cannot belong to \mathbf{W} since they belong to \mathbf{U} and \mathbf{V} respectively. Hence, \mathcal{C} is an active trail in \mathcal{G} .

Suppose now that $X_1 \neq A$. Then, Trail C^* contains Node X_{i-2} , i.e., it contains Subsequence $\langle X_{i-2}, A, L, B \rangle$. If X_{i-2} is a child of A , then Trail $\mathcal{C} = \langle X_1, \dots, X_{i-2}, X_{i-1} = A, X_{i+1} = B, \dots, X_k \rangle$ belongs to both \mathcal{G}^* and \mathcal{G} . In addition, all the nodes in \mathcal{C} have the same type of connection (convergent/non-convergent) as in C^* . Therefore, since $\mathbf{Desc}_{\mathcal{G}}(X) = \mathbf{Desc}_{\mathcal{G}^*}(X)$ for all the nodes $X \in \mathcal{C}$, if C^* is an active trail of \mathcal{G}^* , then \mathcal{C} is an active trail of \mathcal{G} .

Assume now that X_{i-2} is a parent of A . Let $\mathcal{C} = \langle X_1, \dots, X_{i-2}, X_{i+1} = B, \dots, X_k \rangle$. \mathcal{C} is a trail of \mathcal{G} . In addition, all of its nodes have the same type of connection (convergent/non-convergent) in \mathcal{G} as their corresponding node of C^* in \mathcal{G}^* . Therefore, since $\mathbf{Desc}_{\mathcal{G}}(X) = \mathbf{Desc}_{\mathcal{G}^*}(X)$ for all the nodes $X \in \mathcal{C}$, \mathcal{C} is an active trail of \mathcal{G} .

To complete the proof, let us now show that, if there exists an active trail $\mathcal{C} = \langle X_1 = U, \dots, X_k = V \rangle$ in \mathcal{G} , then there also exists an active trail C^* in \mathcal{G}^* .

If $B \notin \mathcal{C}$, then \mathcal{C} also belong to \mathcal{G}^* because the only arcs that belong to \mathcal{G} but not to \mathcal{G}^* are Arcs $Y \rightarrow B$ with $Y \in \mathbf{Pa}_{\mathcal{G}}(A)$. As $\mathbf{Desc}_{\mathcal{G}}(X) = \mathbf{Desc}_{\mathcal{G}^*}(X)$ for all the nodes $X \in \mathcal{C}$, \mathcal{C} is also an active trail in \mathcal{G}^* . Assume now that $B \in \mathcal{C}$. For the same reason as above, if none of the neighbors of B in \mathcal{C} belong to $\mathbf{Pa}_{\mathcal{G}}(A)$, then \mathcal{C} is a trail of \mathcal{G}^* and is also active.

Let i be the index such that $X_i = B$. If some neighbors of B belong to $\mathbf{Pa}_{\mathcal{G}}(A)$, two cases can obtain: case 1) exactly one neighbor of B belongs to $\mathbf{Pa}_{\mathcal{G}}(A)$; and case 2) exactly two neighbors of B belongs to $\mathbf{Pa}_{\mathcal{G}}(A)$. As for case 1), without loss of generality, assume that $X_{i-1} \in \mathbf{Pa}_{\mathcal{G}}(A)$ (else, reverse Trail \mathcal{C}). If $A \notin \mathbf{W}$, then Trail $C^* = \langle X_1, \dots, X_{i-1}, A, X_i = B, \dots, X_k \rangle$ belongs to \mathcal{G}^* . In addition, the type of connection (convergent/non-convergent) of all the nodes in C^* except A are the same as their counterpart in \mathcal{C} . The connection at A is non-convergent and $A \notin \mathbf{W}$, so that A does not block C^* in \mathcal{G}^* . So, overall C^* is an active trail of \mathcal{G}^* . If, now, $A \in \mathbf{W}$, then let $C^* = \langle X_1, \dots, X_{i-1}, A, L, X_i = B, \dots, X_k \rangle$. This is a trail of \mathcal{G}^* for which the type of connection (convergent/non-convergent) of all the nodes in C^* except A and L are the same as their counterpart in \mathcal{C} . The connection at A is convergent and $A \in \mathbf{W}$, so A does not block C^* in \mathcal{G}^* . The connection at L is non-convergent and $L \notin \mathbf{W}$ since $L \notin \mathbf{X}_O$. So L does not block C^* . Consequently, C^* is active in \mathcal{G}^* .

Consider now Case 2), i.e., the two neighbors of B in \mathcal{C} belong to $\mathbf{Pa}_{\mathcal{G}}(A)$. This means that X_{i-1}, B, X_{i+1} form a convergent connection. Since \mathcal{C} is active, either B or some of its descendants belong to \mathbf{W} . But B is a child of A in both \mathcal{G} and \mathcal{G}^* . Therefore, either A or some of its descendants belong to \mathbf{W} . As a consequence, if C^* is the trail obtained from \mathcal{C} by substituting B by A , then the connection at A in C^* is convergent and A does not block C^* . For all the other

⁸ A simple trail is a trail in which no node appears more than once. It is well known that, for any active (resp. blocked) trail between a pair of nodes (X, Y) , there also exists a simple active (resp. blocked) trail between X and Y .

nodes, the connections are similar in \mathcal{C} and \mathcal{C}^* . Hence, \mathcal{C}^* is active in \mathcal{G}^* . This completes the proof. ■

Proof of Proposition 4. Lemma 1 considers pairs of nodes (A, B) such that there exists no directed path from B to A . So, A is not a descendant of B . In addition, in this lemma, there exists no arc between A and B , so A is not a parent of B . So Lemma 1 states that, in \mathcal{G} , every node is independent of its non-descendants given its parents.

Let \mathcal{G} be a DAG maximizing the BIC score. Then it contains no arc $X \rightarrow Y$ such that the graph \mathcal{G}' resulting from the removal of $X \rightarrow Y$ from \mathcal{G} can maximize the BIC score. Indeed, as $|\mathcal{D}| \rightarrow \infty$, Score $S(Y|\mathbf{Pa}_{\mathcal{G}}(Y)) \rightarrow |\mathcal{D}| \times [\mathbf{I}_{P^*}(Y; \mathbf{Pa}_{\mathcal{G}'}(Y) \cup \{X\}) - \mathbf{H}_{P^*}(Y)] - \frac{\log|\mathcal{D}|}{2} \dim(B|\mathbf{Pa}_{\mathcal{G}'}(Y) \cup \{X\})$ (see the proof of Lemma 1). It cannot be the case that $\mathbf{I}_{P^*}(Y; \mathbf{Pa}_{\mathcal{G}'}(Y) \cup \{X\}) < \mathbf{I}_{P^*}(Y; \mathbf{Pa}_{\mathcal{G}}(Y))$ else \mathcal{G} would not maximize the BIC score (since the term in $\log|\mathcal{D}|$ is infinitely smaller than $|\mathcal{D}|$). But, for every probability distribution Q and every U, V, \mathbf{Z} , it always holds that $\mathbf{I}_Q(U; \mathbf{Z} \cup \{V\}) \geq \mathbf{I}_Q(U; \mathbf{Z})$, with equality only if $U \perp\!\!\!\perp_Q V | \mathbf{Z}$. So, necessarily, $\mathbf{I}_{P^*}(Y; \mathbf{Pa}_{\mathcal{G}'}(Y) \cup \{X\}) = \mathbf{I}_{P^*}(Y; \mathbf{Pa}_{\mathcal{G}}(Y))$. As a consequence, we have that:

$$\begin{aligned} & S(Y|\mathbf{Pa}_{\mathcal{G}}(Y)) - S(Y|\mathbf{Pa}_{\mathcal{G}'}(Y)) \\ & \approx \frac{\log|\mathcal{D}|}{2} [\dim(B|\mathbf{Pa}_{\mathcal{G}'}(Y) \cup \{X\}) - \dim(B|\mathbf{Pa}_{\mathcal{G}}(Y))] \\ & \approx \frac{\log|\mathcal{D}|}{2} (|\Omega_X| - 1) \times (|\Omega_Y| - 1) \times (|\Omega_{\mathbf{Pa}_{\mathcal{G}'}(Y)}|) > 0. \end{aligned}$$

Hence \mathcal{G}' cannot maximize the BIC score. So \mathcal{G} is minimal. Overall, by Corollary 4, p. 120, of [14], \mathcal{G} is a minimal I-map. ■

Proof of Proposition 5. Let N_{uvw} denote the number of records in \mathcal{D} such that $U = u$, $V = v$ and $\mathbf{W} = \mathbf{w}$ and let $N_{u\mathbf{w}} = \sum_{v \in \Omega_V} N_{uvw}$, $N_{v\mathbf{w}} = \sum_{u \in \Omega_U} N_{uvw}$ and $N_{\mathbf{w}} = \sum_{u \in \Omega_U} \sum_{v \in \Omega_V} N_{uvw}$.

Let $\dim(U|V, \mathbf{W})$ and $\dim(U|\mathbf{W})$ denote the number of free parameters in the conditional probability tables $P(U|V, \mathbf{W})$ and $P(U|\mathbf{W})$ respectively, i.e., $\dim(U|V, \mathbf{W}) = (|\Omega_U| - 1) \times |\Omega_V| \times |\Omega_{\mathbf{W}}|$ and $\dim(U|\mathbf{W}) = (|\Omega_U| - 1) \times |\Omega_{\mathbf{W}}|$. So, we have that:

$$\Delta_{dim} = \frac{1}{2} \log(|\mathcal{D}|) [\dim(U|V, \mathbf{W}) - \dim(U|\mathbf{W})] = \frac{1}{2} \log(|\mathcal{D}|) \delta,$$

with $\delta = (|\Omega_U| - 1) \times (|\Omega_V| - 1) \times |\Omega_{\mathbf{W}}|$. As a consequence, we have that:

$$\begin{aligned} & S(U|V, \mathbf{W}) - S(U|\mathbf{W}) \\ & = \sum_{u, v, \mathbf{w}} N_{uvw} \left[\log \left(\frac{N_{uvw}}{N_{v\mathbf{w}}} \right) - \log \left(\frac{N_{u\mathbf{w}}}{N_{\mathbf{w}}} \right) \right] - \Delta_{dim} \\ & = \sum_{u, v, \mathbf{w}} N_{uvw} \log \left(\frac{N_{uvw} N_{\mathbf{w}}}{N_{u\mathbf{w}} N_{v\mathbf{w}}} \right) - \Delta_{dim} \end{aligned}$$

So we have that:

$$\begin{aligned} & 2 \times (S(U|V, \mathbf{W}) - S(U|\mathbf{W}) + \Delta_{dim}) \\ & = 2 \sum_{u, v, \mathbf{w}} N_{uvw} \log \left(\frac{N_{uvw} N_{\mathbf{w}}}{N_{u\mathbf{w}} N_{v\mathbf{w}}} \right) = G2(U, V|\mathbf{W}), \end{aligned}$$

where $G2()$ is the formula used in the classical G-test. It is well-known that, when U and V are independent given a set \mathbf{Z} , the $G2$ formula follows a χ^2 distribution of δ degrees of freedom. So, given a risk level α , U and V are judged independent if the value of $f_{BIC}(U, V|\mathbf{Z})$ is lower than the critical value $\chi_{\delta}^2(\alpha)$ of the χ^2 distribution. ■

Proof of Proposition 6. Let n and m denote the number of nodes and arcs of \mathcal{G} respectively. Let k be the maximum number of parents and children of the nodes. Assume that, for conditional independence tests, Algorithm 2 is used and that we limit it to sets \mathbf{Z} such that $|\mathbf{Z}| \leq h$. Then Algorithm 2 completes in $O(nh|\mathcal{D}|)$ time. Indeed, each call to Function f_{BIC} requires parsing the database once, which is performed in $O(|\mathcal{D}|)$ time. As Step 6 examines all the possible Y nodes, its time complexity is $O(n|\mathcal{D}|)$. Finally, the *while* loop of Lines 5–9 is executed at most h times. So, overall, the time complexity of Algorithm 2 is $O(nh|\mathcal{D}|)$.

Now, let us determine the complexity of Algorithm 1. In Graph \mathcal{G} , there exist at most nk^2 triangles (for each node, triangles can be created by selecting two parents). To check whether one is latent (Rule 2), each of its 3 arcs must be examined by Algorithm 2. So Line 2 is completed in $O(n^2 k^2 h |\mathcal{D}|)$ time. On Line 2, the information about which pair of nodes is independent is cached. So, determining their types on Lines 6 and 8 is performed in $O(1)$ time. Determining whether $|\mathbf{Pa}_{\mathcal{G}}(X_3)| \geq 3$ can also be done in $O(1)$. As for Line 8, there are at most $2k$ nodes D to examine (at most k parents and k children), each using Algorithm 2. So, the time complexity of Line 8 is $O(nkh|\mathcal{D}|)$ and, therefore, that of Loop 5–9 is $O(n^2 k^3 h |\mathcal{D}|)$. There are at most nk^2 triangles in \mathcal{G} , hence $O(nk^2)$ iterations of the *for* loop of Lines 10–14. Each instruction on lines 11 to 14 can be performed in $O(1)$ times, hence the loop of Lines 10–14 can be performed in $O(n^2 k^3 h |\mathcal{D}|)$ time. Finally, on Line 15, \mathcal{G} is transformed into a CPDAG, which can be done in time $O(m \log n)$, see [2].

Overall, the time complexity of Algorithm 1 is therefore $O(n^2 k^3 h |\mathcal{D}| + m \log n)$. ■

B Additional experiments

In this section, additional experiments generated similarly to those of Section 4 are performed, highlighting the robustness of our results. In the first two subsections, we vary the number of latent confounders as well as their domain size. The experiments highlight the fact that the results presented in the paper (both recovering the structure and detecting latent confounders) are not sensitive to these features. In the third subsection, we vary the limit on the number of parents required by CPBayes from 4 to 6. The results show that increasing these numbers lead to significant improvements neither in the learning of structures nor in that of latent confounders.

B.1 Detecting multiple/non-Boolean latent confounders

Table 3 reports the learning of the confounders in datasets generated by the Insurance CBN to which we added 2 to 4 latent Boolean confounders. As for the results presented in the paper, whatever the number of latent confounders to be found, Algorithm 1 outperforms MIIC and FCI w.r.t. the wrongly identified confounders and the precision metrics. FCI outperforms the other algorithms w.r.t. the number of correctly identified latent confounders and the recall metrics. As for the F1 metrics, Algorithm 1 and MIIC outperform the other algorithms on large and small datasets respectively.

Table 4 reports the learning of the confounders in datasets generated by the Insurance CBN to which we added two latent confounders with different domain sizes. Here again, the results are similar to those provided in the paper.

$ \mathbf{X}_H $	$ \mathcal{D} $	Algorithm 1						MIIC					FCI				
		ok	¬ok	prec.	recall	F1	time	ok	¬ok	prec.	recall	F1	ok	¬ok	prec.	recall	F1
2	5000	0.20	0.20	0.50	0.10	0.17	0.042	1.62	4.04	0.29	0.81	0.42	1.88	8.86	0.18	0.94	0.30
	10000	0.30	0.28	0.52	0.15	0.23	0.079	1.48	3.32	0.31	0.74	0.44	1.96	8.78	0.18	0.98	0.31
	20000	0.62	0.30	0.67	0.31	0.42	0.172	1.66	3.88	0.30	0.83	0.44	1.94	8.44	0.19	0.97	0.31
	50000	1.16	0.54	0.68	0.58	0.63	0.373	1.78	3.48	0.34	0.89	0.49	1.90	8.66	0.18	0.95	0.30
	100000	1.32	0.72	0.65	0.66	0.65	0.791	1.76	3.00	0.37	0.88	0.52	1.76	8.20	0.18	0.88	0.29
3	5000	0.18	0.16	0.53	0.06	0.11	0.047	2.04	5.20	0.28	0.68	0.40	2.62	9.84	0.21	0.87	0.34
	10000	0.48	0.20	0.71	0.16	0.26	0.088	2.38	5.00	0.32	0.79	0.46	2.86	10.10	0.22	0.95	0.36
	20000	0.96	0.48	0.67	0.32	0.43	0.207	2.08	6.22	0.25	0.69	0.37	2.84	9.90	0.22	0.95	0.36
	50000	1.50	0.52	0.74	0.50	0.60	0.469	2.26	5.96	0.27	0.75	0.40	2.78	8.78	0.24	0.93	0.38
	100000	1.74	0.76	0.70	0.58	0.63	1.383	2.28	5.24	0.30	0.76	0.43	2.60	8.30	0.24	0.87	0.37
4	5000	0.20	0.24	0.45	0.05	0.09	0.057	2.62	6.66	0.28	0.66	0.39	3.56	12.60	0.22	0.89	0.35
	10000	0.40	0.32	0.56	0.10	0.17	0.104	2.70	6.08	0.31	0.68	0.42	3.66	11.24	0.25	0.92	0.39
	20000	1.08	0.34	0.76	0.27	0.40	0.221	3.04	6.04	0.33	0.76	0.46	3.70	11.04	0.25	0.93	0.39
	50000	1.96	0.96	0.67	0.49	0.57	0.588	2.94	6.72	0.30	0.74	0.43	3.68	10.20	0.27	0.92	0.41
	100000	2.16	1.20	0.64	0.54	0.59	1.748	2.90	6.72	0.30	0.73	0.43	3.38	8.74	0.28	0.85	0.42

Table 3: Confounders learnt for Insurance with different numbers of Boolean latent confounders.

$ \Omega_{L_i} $	$ \mathcal{D} $	Algorithm 1						MIIC					FCI				
		ok	¬ok	prec.	recall	F1	time	ok	¬ok	prec.	recall	F1	ok	¬ok	prec.	recall	F1
2	5000	0.20	0.20	0.50	0.10	0.17	0.042	1.62	4.04	0.29	0.81	0.42	1.88	8.86	0.18	0.94	0.30
	10000	0.30	0.28	0.52	0.15	0.23	0.079	1.48	3.32	0.31	0.74	0.44	1.96	8.78	0.18	0.98	0.31
	20000	0.62	0.30	0.67	0.31	0.42	0.172	1.66	3.88	0.30	0.83	0.44	1.94	8.44	0.19	0.97	0.31
	50000	1.16	0.54	0.68	0.58	0.63	0.373	1.78	3.48	0.34	0.89	0.49	1.90	8.66	0.18	0.95	0.30
	100000	1.32	0.72	0.65	0.66	0.65	0.791	1.76	3.00	0.37	0.88	0.52	1.76	8.20	0.18	0.88	0.29
3	5000	0.10	0.20	0.33	0.05	0.09	0.048	1.18	5.16	0.19	0.59	0.28	1.86	10.38	0.15	0.93	0.26
	10000	0.26	0.28	0.48	0.13	0.20	0.091	1.14	3.48	0.25	0.57	0.34	1.74	9.22	0.16	0.87	0.27
	20000	0.62	0.48	0.56	0.31	0.40	0.181	1.50	4.46	0.25	0.75	0.38	1.68	8.86	0.16	0.84	0.27
	50000	0.88	0.62	0.59	0.44	0.50	0.420	1.48	4.16	0.26	0.74	0.39	1.68	8.82	0.16	0.84	0.27
	100000	1.10	0.78	0.59	0.55	0.57	1.108	1.32	4.46	0.23	0.66	0.34	1.54	7.18	0.18	0.77	0.29
4	5000	0.20	0.24	0.45	0.10	0.16	0.051	1.34	5.46	0.20	0.67	0.30	1.86	11.32	0.14	0.93	0.25
	10000	0.28	0.26	0.52	0.14	0.22	0.097	1.42	4.80	0.23	0.71	0.35	1.82	10.10	0.15	0.91	0.26
	20000	0.50	0.36	0.58	0.25	0.35	0.197	1.42	4.58	0.24	0.71	0.36	1.66	9.74	0.15	0.83	0.25
	50000	0.84	0.64	0.57	0.42	0.48	0.442	1.32	5.50	0.19	0.66	0.30	1.64	8.82	0.16	0.82	0.26
	100000	1.08	0.60	0.64	0.54	0.59	1.121	1.52	6.50	0.19	0.76	0.30	1.62	8.44	0.16	0.81	0.27

Table 4: Confounders learnt for Insurance with latent confounders with different domain sizes.

B.2 The quality of the CPDAGs

Table 5 compares the CPDAGs learnt by Algorithm 1, MIIC and FCI with those of the CBNs that generated the datasets. These CBNs correspond to Insurance to which we added 2 to 4 Boolean latent confounders. As for the results presented in the paper, Algorithm 1 outperforms MIIC and FCI in terms of the number of arcs/edges learnt correctly as well as in terms of the incorrect types of edges/arcs (undirected edges (resp. arcs) of the generating CBN learnt as arcs (resp. edges)) and in terms of the edges/arcs learnt in excess (the original CBN contains neither an edge nor an arc for the pairs of nodes concerned). FCI outperforms the other algorithms in terms of arcs reversed. MIIC is the best in terms of missed arcs/edges.

Table 6 reports the results of experiments in which the datasets were generated from Insurance with two latent confounders. Here, the domain sizes of these confounders vary from 2 to 4.

B.3 The impact of the parents number’s limit of CPBayes

In the experiments section of the paper, the first step of Algorithm 1 is performed by CPBayes [26]. As such, CPBayes takes as input so-called *instances* that are computed from Datasets \mathcal{D} . These contain

all the possible nodes’ sets that CPBayes will consider as potential parent sets and, to control the combinatorial explosion, this requires limiting the number of possible parents of the nodes. In the experiments of Section 4, we set this limit to 4. In the literature, people also fix it to 5 or 6, see, e.g., [27] or [24]. This makes sense because, in classical Bayesian networks, nodes seldom have more than 6 parents. In addition, in practical situations, the number of parents that can be possibly learnt is limited by the size of the dataset (e.g., to be meaningful, independence tests require contingency tables much smaller than the dataset size). Tables 7 and 8 show the impact of these limits on the determination of the latent confounder and on the learnt structure respectively. In these tables columns “N:#” report the results obtained by limiting CPBayes instances to have at most # parents. As can be observed, there is no noticeable difference increasing the limit from 4 to 6. This is probably due to the fact that the benchmark Bayesian networks (child, water, insurance) that generated the datasets have at most 4 parents.

$ \mathbf{X}_H $	$ \mathcal{D} $	Algorithm 1					MIIC					FCI				
		ok	miss	rev.	type	xs	ok	miss	rev.	type	xs	ok	miss	rev.	type	xs
2	5000	32.38	14.44	2.46	6.72	3.82	29.20	12.70	3.60	10.50	12.44	23.90	21.60	0.46	10.04	18.06
	10000	34.68	12.22	2.38	6.72	4.06	29.86	11.70	3.52	10.92	11.46	25.76	18.64	0.30	11.30	17.72
	20000	38.76	9.20	3.34	4.70	5.04	30.42	10.00	3.74	11.84	13.12	27.98	16.18	0.14	11.70	17.08
	50000	41.08	7.58	4.42	2.92	6.42	31.32	8.34	4.00	12.34	12.94	29.42	13.92	0.10	12.56	17.70
	100000	40.34	7.08	4.94	3.64	7.48	31.46	7.88	3.88	12.78	13.40	31.36	12.64	0.12	11.88	16.96
3	5000	33.52	15.46	1.70	7.32	3.70	31.94	12.08	5.24	8.74	17.16	27.34	21.44	1.60	7.62	20.08
	10000	34.72	13.38	2.54	7.36	4.86	33.80	10.00	5.74	8.46	17.38	29.62	19.08	1.20	8.10	20.62
	20000	37.84	10.08	3.36	6.72	6.88	32.64	9.14	5.58	10.64	21.94	31.94	16.08	0.84	9.14	20.12
	50000	40.42	8.54	4.28	4.76	8.36	35.26	7.80	4.92	10.02	23.24	34.00	13.18	0.72	10.10	18.20
	100000	41.76	7.66	4.54	4.04	10.10	35.70	7.66	4.12	10.52	21.32	35.84	11.82	0.42	9.92	17.74
4	5000	33.86	16.08	1.84	8.22	4.34	33.66	11.28	6.56	8.50	20.42	29.10	23.06	1.80	6.04	25.46
	10000	34.44	14.52	2.36	8.68	5.72	35.54	9.96	6.36	8.14	21.82	32.80	19.30	1.54	6.36	22.80
	20000	38.54	11.78	3.40	6.28	7.74	36.70	8.40	5.70	9.20	22.66	33.66	17.00	0.64	8.70	22.62
	50000	40.34	9.50	4.68	5.48	11.74	36.04	7.98	5.98	10.00	26.80	36.60	14.04	0.48	8.88	21.30
	100000	37.84	8.94	5.38	7.84	13.60	37.94	7.34	6.96	7.76	29.02	39.92	12.28	1.04	6.76	19.04

Table 5: Comparisons of the learnt CPDAGs with those of the CBNs (with confounders) that generated the datasets in function of the number of the CBN’s latent confounders.

$ \Omega_{L_i} $	$ \mathcal{D} $	Algorithm 1					MIIC					FCI				
		ok	miss	rev.	type	xs	ok	miss	rev.	type	xs	ok	miss	rev.	type	xs
2	5000	32.38	14.44	2.46	6.72	3.82	29.20	12.70	3.60	10.50	12.44	23.90	21.60	0.46	10.04	18.06
	10000	34.68	12.22	2.38	6.72	4.06	29.86	11.70	3.52	10.92	11.46	25.76	18.64	0.30	11.30	17.72
	20000	38.76	9.20	3.34	4.70	5.04	30.42	10.00	3.74	11.84	13.12	27.98	16.18	0.14	11.70	17.08
	50000	41.08	7.58	4.42	2.92	6.42	31.32	8.34	4.00	12.34	12.94	29.42	13.92	0.10	12.56	17.70
	100000	40.34	7.08	4.94	3.64	7.48	31.46	7.88	3.88	12.78	13.40	31.36	12.64	0.12	11.88	16.96
3	5000	34.74	13.78	1.76	5.72	2.90	28.76	11.58	3.30	12.36	15.88	23.02	21.40	0.64	10.94	21.04
	10000	38.00	11.86	1.96	4.18	3.58	29.22	11.04	3.04	12.70	12.42	25.84	18.54	0.22	11.40	18.90
	20000	40.16	9.26	3.16	3.42	5.24	30.20	9.20	3.62	12.98	15.58	27.86	16.16	0.28	11.70	18.36
	50000	41.76	7.72	3.92	2.60	6.54	30.48	8.12	3.66	13.74	16.40	29.42	14.24	0.22	12.12	18.24
	100000	40.84	7.32	4.42	3.42	8.04	31.68	7.42	3.36	13.54	18.24	31.98	11.40	0.12	12.50	15.52
4	5000	34.22	13.28	1.88	6.62	3.00	27.28	11.42	3.80	13.50	16.38	22.18	22.06	0.68	11.08	22.90
	10000	39.72	10.86	2.04	3.38	3.44	30.38	9.70	3.64	12.28	15.70	25.20	18.12	0.38	12.30	20.52
	20000	39.92	9.06	2.94	4.08	5.08	29.80	8.44	4.00	13.76	17.18	26.92	16.22	0.24	12.62	20.18
	50000	42.38	7.86	3.88	1.88	7.08	30.58	7.78	3.70	13.94	20.40	29.52	13.28	0.16	13.04	18.46
	100000	42.24	6.74	4.26	2.76	7.92	30.76	6.52	4.64	14.08	25.40	31.16	11.96	0.14	12.74	17.90

Table 6: Comparisons of the learnt CPDAGs with those of the CBNs (with 2 latent confounders) that generated the datasets, in function of the domain sizes of the CBN’s latent confounders.

CBN	$ \mathcal{D} $	ok			\neg ok			precision			recall			F1			time		
		N:4	N:5	N:6	N:4	N:5	N:6	N:4	N:5	N:6	N:4	N:5	N:6	N:4	N:5	N:6	N:4	N:5	N:6
child	5000	0.50	0.50	0.50	0.06	0.06	0.06	0.89	0.89	0.89	0.25	0.25	0.25	0.39	0.39	0.39	0.014	0.013	0.016
	10000	0.76	0.76	0.76	0.18	0.18	0.18	0.81	0.81	0.81	0.38	0.38	0.38	0.52	0.52	0.52	0.028	0.029	0.027
	20000	1.10	1.10	1.10	0.12	0.12	0.12	0.90	0.90	0.90	0.55	0.55	0.55	0.68	0.68	0.68	0.050	0.068	0.059
	50000	1.42	1.44	1.44	0.14	0.12	0.12	0.91	0.92	0.92	0.71	0.72	0.72	0.80	0.81	0.81	0.103	0.119	0.130
	100000	1.44	1.44	1.44	0.14	0.14	0.14	0.91	0.91	0.91	0.72	0.72	0.72	0.80	0.80	0.80	0.190	0.223	0.225
water	5000	0.16	0.16	0.16	1.56	1.56	1.56	0.09	0.09	0.09	0.08	0.08	0.08	0.09	0.09	0.09	0.017	0.022	0.016
	10000	0.44	0.44	0.44	0.04	0.04	0.04	0.92	0.92	0.92	0.22	0.22	0.22	0.35	0.35	0.35	0.043	0.050	0.050
	20000	0.80	0.80	0.80	0.22	0.22	0.22	0.78	0.78	0.78	0.40	0.40	0.40	0.53	0.53	0.53	0.104	0.131	0.120
	50000	1.16	1.16	1.16	0.60	0.60	0.60	0.66	0.66	0.66	0.58	0.58	0.58	0.62	0.62	0.62	0.132	0.157	0.159
	100000	1.22	1.22	1.22	1.04	1.04	1.04	0.54	0.54	0.54	0.61	0.61	0.61	0.57	0.57	0.57	0.248	0.333	0.318
insurance	5000	0.20	0.20	0.20	0.20	0.20	0.20	0.50	0.50	0.50	0.10	0.10	0.10	0.17	0.17	0.17	0.042	0.044	0.042
	10000	0.30	0.30	0.30	0.28	0.28	0.28	0.52	0.52	0.52	0.15	0.15	0.15	0.23	0.23	0.23	0.079	0.086	0.090
	20000	0.62	0.60	0.60	0.30	0.34	0.34	0.67	0.64	0.64	0.31	0.30	0.30	0.42	0.41	0.41	0.172	0.192	0.198
	50000	1.16	1.14	1.14	0.54	0.42	0.42	0.68	0.73	0.73	0.58	0.57	0.57	0.63	0.64	0.64	0.373	0.429	0.419
	100000	1.32	1.32	1.32	0.72	0.54	0.54	0.65	0.71	0.71	0.66	0.66	0.66	0.65	0.68	0.68	0.791	1.009	0.994

Table 7: Confounders found for different limits on the number of parents used by CPBayes.

CBN	D	ok			miss			reversed			type			excess		
		N:4	N:5	N:6	N:4	N:5	N:6	N:4	N:5	N:6	N:4	N:5	N:6	N:4	N:5	N:6
child	5000	22.46	22.46	22.46	3.08	3.08	3.08	1.02	1.02	1.02	2.44	2.44	2.44	2.54	2.54	2.54
	10000	23.10	23.10	23.10	2.52	2.52	2.52	1.52	1.52	1.52	1.86	1.86	1.86	3.12	3.12	3.12
	20000	22.88	22.88	22.88	1.84	1.84	1.84	2.22	2.22	2.22	2.06	2.06	2.06	3.62	3.64	3.64
	50000	22.98	22.98	22.98	1.22	1.18	1.18	2.84	2.88	2.88	1.96	1.96	1.96	4.34	4.36	4.36
	100000	23.20	23.20	23.20	1.14	1.14	1.14	2.88	2.88	2.88	1.78	1.78	1.78	4.50	4.56	4.56
water	5000	16.72	16.72	16.72	40.18	40.18	40.18	4.72	4.72	4.72	8.38	8.38	8.38	4.60	4.60	4.60
	10000	19.00	19.00	19.00	36.98	36.98	36.98	7.58	7.58	7.58	6.44	6.44	6.44	5.96	5.96	5.96
	20000	21.12	21.12	21.12	36.64	36.64	36.64	6.82	6.82	6.82	5.42	5.42	5.42	8.72	8.72	8.72
	50000	26.22	26.22	26.22	32.48	32.48	32.48	7.20	7.20	7.20	4.10	4.10	4.10	7.02	7.02	7.02
	100000	29.94	29.94	29.94	29.42	29.42	29.42	7.10	7.10	7.10	3.54	3.54	3.54	7.06	7.06	7.06
insurance	5000	32.38	32.38	32.38	14.44	14.44	14.44	2.46	2.46	2.46	6.72	6.72	6.72	3.82	3.82	3.82
	10000	34.68	34.68	34.68	12.22	12.22	12.22	2.38	2.38	2.38	6.72	6.72	6.72	4.06	4.06	4.06
	20000	38.76	38.76	38.76	9.20	9.24	9.24	3.34	3.30	3.30	4.70	4.70	4.70	5.04	5.04	5.04
	50000	41.08	41.56	41.56	7.58	7.60	7.60	4.42	4.26	4.26	2.92	2.58	2.58	6.42	6.06	6.06
	100000	40.34	41.06	41.06	7.08	7.08	7.08	4.94	4.76	4.76	3.64	3.10	3.10	7.48	6.90	6.90

Table 8: Comparisons of the learnt CPDAGs with those of the CBNs (with confounders) that generated the datasets.

C Converting a causal model into a Bayesian network

In this section, we show on an example how to convert a causal model, as defined in Definition 1 of the paper, into a Bayesian network. For this purpose, consider the causal model of Figure 5, where $\mathbf{X} = \{A, B, C, D, E, F\}$. The domain sizes of all the random disturbances ξ_i are equal to $\{1, 2, 3, 4\}$. Those of the variables of \mathbf{X} will be clearly identified from their assigned parameters.

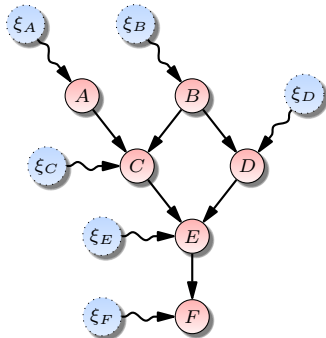


Figure 5: The structure of a causal model.

The probability distributions of the random disturbances are defined as follows:

$$P(\xi_A) = \begin{bmatrix} 0.2 & 0.1 & 0.3 & 0.4 \end{bmatrix}$$

$$P(\xi_B) = \begin{bmatrix} 0.2 & 0.4 & 0.3 & 0.1 \end{bmatrix}$$

$$P(\xi_C) = \begin{bmatrix} 0.3 & 0.3 & 0.2 & 0.2 \end{bmatrix}$$

$$P(\xi_D) = \begin{bmatrix} 0.5 & 0.3 & 0.1 & 0.1 \end{bmatrix}$$

$$P(\xi_E) = \begin{bmatrix} 0.1 & 0.2 & 0.3 & 0.4 \end{bmatrix}$$

$$P(\xi_F) = \begin{bmatrix} 0.2 & 0.3 & 0.3 & 0.2 \end{bmatrix}$$

Definition 1 of the paper refers to Definition 2.2.2 from [15]. As such, the parameters f_i assigned to the variables of \mathbf{X} are deterministic functions (see [15, p. 68]). In our example, the parameters of the causal model are the following:

$$f_A(\xi_A) = \begin{cases} a_1 & \text{if } \xi_A \leq 2, \\ a_2 & \text{otherwise} \end{cases}$$

$$f_B(\xi_B) = \begin{cases} b_1 & \text{if } \xi_B \bmod 2 = 0, \\ b_2 & \text{otherwise} \end{cases}$$

$$f_C(A, B, \xi_C) = \begin{cases} A & \text{if } \xi_C \leq 2, \\ B & \text{otherwise} \end{cases}$$

$$f_D(B, \xi_D) = \begin{cases} d_1 & \text{if } B = b_1 \text{ and } \xi_D \bmod 2 = 1, \\ d_2 & \text{if } B = b_2 \text{ and } \xi_D = 2, \\ d_3 & \text{otherwise} \end{cases}$$

$$f_E(C, D, \xi_E) = \begin{cases} e_1 & \text{if } C \in \{a_1, b_1\} \text{ and } \xi_E \leq 2, \\ e_2 & \text{if } C \in \{a_2, b_2\} \text{ and } D = d_2, \\ e_3 & \text{otherwise} \end{cases}$$

$$f_F(E, \xi_F) = \begin{cases} f_1 & \text{if } \xi_F = 1, \\ f_2 & \text{if } E \in \{e_1, e_3\} \text{ and } \xi_F = 2, \\ f_3 & \text{otherwise} \end{cases}$$

Deterministic functions like those above can be equivalently represented as conditional probability tables (CPT) such that: i) the variables on the right side of the conditioning bar are those over which the function is defined; ii) the variable on the left side of the conditioning bar is the one corresponding to the codomain of the function; iii) the values in the CPT are either 1 or 0, depending on whether the value of the variable on the left side of the conditioning bar corresponds or not to the value of the function given those of the variables at the right side of the conditioning bar. Therefore, the above deterministic functions can be represented as:

$$P(A|\xi_A) =$$

$A \setminus \xi_A$	1	2	3	4
a_1	1	1	0	0
a_2	0	0	1	1

$$P(B|\xi_B) =$$

$B \setminus \xi_B$	1	2	3	4
b_1	0	1	0	1
b_2	1	0	1	0

$$P(C|A, B, \xi_C) =$$

	a_1				a_2											
	b_1		b_2		b_1		b_2									
$C \setminus \xi_C$	1	2	3	4	1	2	3	4	1	2	3	4	1	2	3	4
a_1	1	1	0	0	1	1	0	0	0	0	0	0	0	0	0	0
a_2	0	0	0	0	0	0	0	0	1	1	0	0	1	1	0	0
b_1	0	0	1	1	0	0	0	0	0	0	1	1	0	0	0	0
b_2	0	0	0	0	0	0	1	1	0	0	0	0	0	0	1	1

$$P(D|B, \xi_D) =$$

	b_1		b_2					
$D \setminus \xi_D$	1	2	3	4	1	2	3	4
d_1	1	0	1	0	0	0	0	0
d_2	0	0	0	0	0	1	0	0
d_3	0	1	0	1	1	0	1	1

$$P(E|C, D, \xi_E) =$$

	a_1				a_2																			
	d_1		d_2		d_3		d_1		d_2		d_3													
$E \setminus \xi_E$	1	2	3	4	1	2	3	4	1	2	3	4	1	2	3	4	1	2	3	4				
e_1	1	1	0	0	1	1	0	0	1	1	0	0	0	0	0	0	0	0	0	0	0			
e_2	0	0	0	0	0	0	0	0	0	0	0	0	0	0	0	0	1	1	1	1	0	0	0	0
e_3	0	0	1	1	0	0	1	1	0	0	1	1	1	1	1	1	0	0	0	0	1	1	1	1

	b_1				b_2																			
	d_1		d_2		d_3		d_1		d_2		d_3													
$E \setminus \xi_E$	1	2	3	4	1	2	3	4	1	2	3	4	1	2	3	4	1	2	3	4				
e_1	1	1	0	0	1	1	0	0	1	1	0	0	0	0	0	0	0	0	0	0	0	0	0	0
e_2	0	0	0	0	0	0	0	0	0	0	0	0	0	0	0	0	1	1	1	1	0	0	0	0
e_3	0	0	1	1	0	0	1	1	0	0	1	1	1	1	1	1	0	0	0	0	1	1	1	1

$$P(F|E, \xi_F) =$$

	e_1		e_2		e_3							
$F \setminus \xi_F$	1	2	3	4	1	2	3	4	1	2	3	4
f_1	1	0	0	0	1	0	0	0	1	0	0	0
f_2	0	1	0	0	0	0	0	0	0	1	0	0
f_3	0	0	1	1	0	1	1	1	0	0	1	1

All the above probability distributions, together with the structure of Figure 6.a, form the Bayesian network corresponding to the causal model of Figure 5. Unfortunately, this Bayesian network still includes the disturbance nodes whereas the one that we are looking for is that of Figure 6.b. Fortunately, it is easy to remove these disturbance variables: it is sufficient to marginalize them out from the joint distribution of the Bayesian network of Figure 6.a, as shown below.

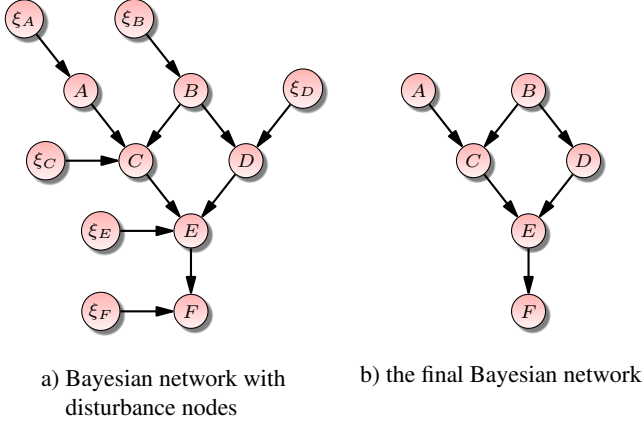


Figure 6: The Bayesian networks corresponding to the causal model.

Let \mathcal{G} and Ξ denote the graph of Figure 6.b and Set $\{\xi_A, \xi_B, \xi_C, \xi_D, \xi_E, \xi_F\}$ respectively. Then the joint distribution of the Bayesian network of Figure 6.a is equal to:

$$P(\mathbf{X}, \Xi) = \prod_{X \in \mathbf{X}} P(\xi_X) \times P(X | \mathbf{Pa}_{\mathcal{G}}(X), \xi_X),$$

and marginalizing out the disturbance variables corresponds to computing:

$$\begin{aligned} P(\mathbf{X}) &= \sum_{\xi \in \Xi} \prod_{X \in \mathbf{X}} P(\xi_X) \times P(X | \mathbf{Pa}_{\mathcal{G}}(X), \xi_X), \\ &= \prod_{X \in \mathbf{X}} \sum_{\xi_X} P(\xi_X) \times P(X | \mathbf{Pa}_{\mathcal{G}}(X), \xi_X) \\ &= \prod_{X \in \mathbf{X}} P(X | \mathbf{Pa}_{\mathcal{G}}(X)), \end{aligned}$$

which corresponds to the decomposition of Figure 6.b. Therefore, for each variable X in \mathbf{X} , we just need to multiply the CPT of X by the probability distribution of ξ_X and, then, marginalize out ξ_X . This results in the following computations, which can also be found in the jupyter notebook at <https://pageperso.lis-lab.fr/christophe.gonzales/research/notebooks/ecai2024.ipynb>:

$$\begin{aligned} P(A, \xi_A) &= P(A | \xi_A) \times P(\xi_A) \\ &= \begin{array}{c|cccc} A \backslash \xi_A & 1 & 2 & 3 & 4 \\ \hline a_1 & 0.2 & 0.1 & 0.0 & 0.0 \\ a_2 & 0.0 & 0.0 & 0.3 & 0.4 \end{array} \end{aligned}$$

Hence, marginalizing out ξ_A , we have that:

$$\begin{aligned} P(A) &= \sum_{\xi_A} P(A, \xi_A) \\ &= \begin{array}{c|c} a_1 & 0.3 \\ \hline a_2 & 0.7 \end{array} \end{aligned}$$

Similarly, we have that:

$$\begin{aligned} P(B) &= \sum_{\xi_B} P(B | \xi_B) \times P(\xi_B) \\ &= \sum_{\xi_B} \begin{array}{c|cccc} B \backslash \xi_B & 1 & 2 & 3 & 4 \\ \hline b_1 & 0.0 & 0.4 & 0.0 & 0.1 \\ b_2 & 0.2 & 0.0 & 0.3 & 0.0 \end{array} \\ &= \begin{array}{c|c} b_1 & 0.5 \\ \hline b_2 & 0.5 \end{array} \end{aligned}$$

$$P(D, \xi_D | B) = P(D | B, \xi_D) \times P(\xi_D)$$

	b_1				b_2			
$D \backslash \xi_D$	1	2	3	4	1	2	3	4
d_1	0.5	0.0	0.1	0.0	0.0	0.0	0.0	0.0
d_2	0.0	0.0	0.0	0.0	0.0	0.3	0.0	0.0
d_3	0.0	0.3	0.0	0.1	0.5	0.0	0.1	0.1

So we have that:

$$\begin{aligned} P(D | B) &= \sum_{\xi_D} P(D, \xi_D | B) \\ &= \begin{array}{c|cc} D \backslash B & b_1 & b_2 \\ \hline d_1 & 0.6 & 0.0 \\ d_2 & 0.0 & 0.3 \\ d_3 & 0.4 & 0.7 \end{array} \end{aligned}$$

For variables C , E and F , the tables, which are large, are provided on the next page.

$$P(C, \xi_C | A, B) = P(C | A, B, \xi_C) \times P(\xi_C)$$

$C \setminus \xi_C$	a_1								a_2							
	b_1				b_2				b_1				b_2			
	1	2	3	4	1	2	3	4	1	2	3	4	1	2	3	4
a_1	0.3	0.3	0.0	0.0	0.3	0.3	0.0	0.0	0.0	0.0	0.0	0.0	0.0	0.0	0.0	0.0
a_2	0.0	0.0	0.0	0.0	0.0	0.0	0.0	0.0	0.3	0.3	0.0	0.0	0.3	0.3	0.0	0.0
b_1	0.0	0.0	0.2	0.2	0.0	0.0	0.0	0.0	0.0	0.0	0.2	0.2	0.0	0.0	0.0	0.0
b_2	0.0	0.0	0.0	0.0	0.0	0.0	0.2	0.2	0.0	0.0	0.0	0.0	0.0	0.0	0.2	0.2

So we have that:

$$P(C | A, B) = \sum_{\xi_C} P(C, \xi_C | A, B)$$

$C \setminus B$	a_1		a_2	
	b_1	b_2	b_1	b_2
a_1	0.6	0.6	0.0	0.0
a_2	0.0	0.0	0.6	0.6
b_1	0.4	0.0	0.4	0.0
b_2	0.0	0.4	0.0	0.4

Similarly, we have that:

$$P(E | C, D) = \sum_{\xi_E} P(E | C, D, \xi_E) \times P(\xi_E)$$

$E \setminus D$	a_1			a_2			b_1			b_2		
	d_1	d_2	d_3	d_1	d_2	d_3	d_1	d_2	d_3	d_1	d_2	d_3
e_1	0.3	0.3	0.3	0.0	0.0	0.0	0.3	0.3	0.3	0.0	0.0	0.0
e_2	0.0	0.0	0.0	0.0	1.0	0.0	0.0	0.0	0.0	0.0	1.0	0.0
e_3	0.7	0.7	0.7	1.0	0.0	1.0	0.7	0.7	0.7	1.0	0.0	1.0

Finally, we have that:

$$P(F, \xi_F | E) = P(F | E, \xi_F) \times P(\xi_F)$$

$F \setminus \xi_F$	e_1				e_2				e_3			
	1	2	3	4	1	2	3	4	1	2	3	4
f_1	0.2	0.0	0.0	0.0	0.2	0.0	0.0	0.0	0.2	0.0	0.0	0.0
f_2	0.0	0.3	0.0	0.0	0.0	0.0	0.0	0.0	0.0	0.3	0.0	0.0
f_3	0.0	0.0	0.3	0.2	0.0	0.3	0.3	0.2	0.0	0.0	0.3	0.2

So:

$$P(F | E) = \sum_{\xi_F} P(F, \xi_F | E)$$

$F \setminus E$	e_1	e_2	e_3
f_1	0.2	0.2	0.2
f_2	0.3	0.0	0.3
f_3	0.5	0.8	0.5